

# CHALMERS



## Resonant Ring Array Antenna Element Study

*Master's Thesis in Wireless, Photonics and Space Engineering*

UNAI ALBISU ARRIETA

RUAG Space AB Sweden & Signals and Systems

Antenna Department

CHALMERS UNIVERSITY OF TECHNOLOGY

Gothenburg, Sweden 2016

Master's Thesis



## **Abstract**

The work carried out in this Master's thesis focuses on the design of an antenna element using HFSS, a commercial software widely used for Electromagnetic simulations in Antenna Engineering and RF design. The work done for this Master's Thesis is based on an Antenna Element design made in RUAG Space AB Sweden twenty years ago, in 1998. The antenna was designed for radio occultation measurements for the GPS frequencies. The goal of the Master thesis is to design a similar antenna but for the Galileo Navigation System frequency bands.

The work has been performed following different steps. First a thorough literature research of the previous design has been done, using the literature provided by RUAG Space AB Sweden. Following this study a complete re-design of the previous antenna has been done in HFSS. Once this step has been made, the antenna for the new requirements has been designed, using the previous design as an starting point. Finally, the study of the mechanical construction of the antenna has been done.



## Acknowledgements

I would like to thank first my two supervisors during this semester, Jian Yang and Johan Wettergren. Their advices at any moment I needed were of incalculable help. Their knowledge and experience was very helpful. Without their help it would be impossible to carry out the work.

I would also like to thank to Ansys Electromagnetics to give me the chance to work with HFSS. Without their contribution this work could not be done.

Thanks also to all the people in RUAG Space AB Sweden for all the help during this semester. All the people I have met there were very kind and helpful, and were able to help me at any time I wanted.

I would also like to thank all my friends in Sweden for their support in the Scandinavian adventure that started two years ago. Without their help and support this adventure would not be as exciting as it has been I would also like to thank all my friends from the Basque Country. Even if they were many kilometres away from me, they have been indispensable for me.

Finally, last but not least, I would like to thank all my family for all the support they have given me ever since I started school until this years in Sweden. Without their support this could not be possible.

Unai Albisu Arrieta, Gothenburg 2016/4/27



# Contents

|          |   |           |
|----------|---|-----------|
| <b>1</b> | <b>Introduction</b>                                       | <b>1</b>  |
| 1.1      | Antenna Specifications . . . . .                          | 1         |
| 1.2      | RUAG Space AB Sweden . . . . .                            | 2         |
| 1.3      | Ansys HFSS . . . . .                                      | 2         |
| 1.4      | Radio Occultation Measurements . . . . .                  | 3         |
| 1.5      | Research Activities on UWB antennas at Chalmers . . . . . | 3         |
| <b>2</b> | <b>Theory</b>   | <b>5</b>  |
| 2.1      | Future Prediction . . . . .                               | 5         |
| 2.2      | Different Antenna options . . . . .                       | 6         |
| 2.2.1    | Single Helix Antenna . . . . .                            | 6         |
| 2.2.2    | Linear Array of Helix Antennas . . . . .                  | 7         |
| 2.2.3    | Array of Large PEC Elements . . . . .                     | 7         |
| 2.2.4    | Printed Resonant Ring Array . . . . .                     | 8         |
| 2.2.5    | Metalized Resonant Ring Array . . . . .                   | 9         |
| 2.2.6    | Conclusions . . . . .                                     | 10        |
| 2.3      | Resonant Ring Array . . . . .                             | 11        |
| 2.3.1    | General Antenna Description . . . . .                     | 11        |
| 2.3.2    | Cavity . . . . .  | 12        |
| 2.3.3    | Resonator Rings . . . . .                                 | 13        |
| 2.3.4    | Slots . . . . .   | 14        |
| 2.3.5    | Feeding Network . . . . .                                 | 18        |
| 2.3.6    | Ground plane, Screw, Spacing and Posts . . . . .          | 18        |
| <b>3</b> | <b>Redesign Old Antenna</b>                               | <b>20</b> |
| 3.1      | High Frequency Slot . . . . .                             | 20        |
| 3.1.1    | Design Method . . . . .                                   | 22        |
| 3.2      | Low Frequency Slot . . . . .                              | 24        |
| 3.3      | Double Excitation . . . . .                               | 26        |
| 3.3.1    | Miter . . . . .   | 26        |

|          |                                   |           |
|----------|-----------------------------------|-----------|
| 3.4      | HF double excitation . . . . .    | 28        |
| 3.5      | LF double excitation . . . . .    | 31        |
| 3.6      | Everything together . . . . .     | 33        |
| <b>4</b> | <b>Improve the bandwidth</b>      | <b>38</b> |
| 4.1      | Double Stub Matching . . . . .    | 38        |
| 4.2      | Adding a patch . . . . .          | 44        |
| 4.3      | Adding a third ring . . . . .     | 48        |
| 4.4      | Same ring for L2 and L5 . . . . . | 57        |
| <b>5</b> | <b>New Antenna Design</b>         | <b>58</b> |
| 5.1      | L5 Excitation . . . . .           | 58        |
| 5.2      | Design lambda/4 line . . . . .    | 67        |
| 5.3      | Final Design . . . . .            | 73        |
| 5.4      | Conclusions . . . . .             | 79        |
|          | <b>Bibliography</b>               | <b>82</b> |

# 1

## Introduction

**A**NTENNA design is nowadays a major concern in Electrical Engineering. Antennas are used in many applications other than traditional communication systems, such as, medicine, meteorology, automation and more. The antenna that has been studied in this project has not been designed for any specific application. Instead, the goal of the master's thesis is to study an antenna that might be interesting for future upcoming applications. The design has been done using Ansys Electromagnetics HFSS design suite. Our efforts have been centered in the design of the feeding network which is the main challenge of the thesis. As has been said before, the design is based on a previous design made in RUAG Space AB Sweden. This design was used for radio occultation measurements, an application that will be explained in this introductory part. The lack of accurate design documentation has driven us to re-design the old antenna in HFSS, making use of the documentation available. In this first introductory part, the reader will be introduced to some fundamental content that will be important to understand the work done in the Master's thesis project. For that, first, the antenna specifications will be presented. Thus, the company where the thesis was done will be introduced. In the following section a brief introduction to the used electromagnetic simulation software will be given. Afterwards, the term radio occultation measurement will be explained as an example of applications using this antennas. Finally, the antenna department of Chalmers will be presented, explaining what work is done there.

### 1.1 Antenna Specifications

The antenna that is wanted to be designed in this thesis project is a resonant ring antenna. The purpose of the antenna is to be able to work in three frequency bands, L1, L2 and L5. This frequency bands are written below,

- L1: 1565-1614MHz

- L2: 1217-1257MHz
- L5: 1145-1245MHz

So, the goal of the thesis will be to study an antenna that was designed for the L1 and L2 bands, and see if it is suitable for the new design. In order to do so, several different designs were tried. The previous design was composed by two resonant rings, each for the respective frequency band. Those resonant rings were excited by slots and the slot was excited by their respective feeding network. The goal of the thesis is to study the previous design and see if it is suitable for the new requirements.

## 1.2 RUAG Space AB Sweden

RUAG Space AB in Sweden specializes in highly reliable on-board satellite equipment including computer systems, antennas and microwave electronics and adapters and separation systems for space launchers[1]. Previously known as Saab Ericsson Aerospace, it was renamed as RUAG Space AB Sweden in 2008. RUAG Space AB Sweden or back in the days Saab Ericsson Aerospace, is well known for its high quality and reliable designs for Space applications. The company has worked with many companies, as well as institutions, such as the European Space Agency or the NASA, along its history. It has taken part in many Space Projects, some of them with high media resonance, for instance, the Rosetta mission, in which RUAG Space took an important role, designing some of the components[2]. For instance, the Rosina (Rosetta Orbiter Spectrometer for Ion and Neutral Analysis) instrument, which features a high-resolution mass spectrometer that was built by RUAG on behalf of the University of Bern and goes by the name of DFMS (Double Focussing Mass Spectrometer) or the high performance communication system.

## 1.3 Ansys HFSS

Ansys HFSS is a industry standard for simulating 3D, full wave, electromagnetic fields[3]. HFSS is a highly precise comercial software for electromagnetic wave simulation. It uses the Finite Element Method to solve the simulations. HFSS has been the main software that has been used during this Master's thesis project. All from the 3-D design to the simulation has been done using the HFSS electromagnetic simulator.

Ansys HFSS uses the finite element method, as said before, to solve the Maxwell's equations inside a certain geometry. It is widely used for antenna design as well as for complex RF electronics circuit element design, including filters, transmission lines and packaging.

## 1.4 Radio Occultation Measurements

The antenna that is going to be designed might be used for applications similar to radio occultation measurements. This is the reason why this application is explained. Radio occultation (RO) is a remote sensing technique used for measuring the physical properties of a planetary atmosphere[4]. The principle relies on the bending that electromagnetic waves suffer when they pass through the earth's atmosphere. This bending is greater or smaller depending on several factors of the atmosphere, such as, temperature, vapor content or pressure. In radio occultation measurement technologies, the bending angle can be calculated, as we know the GPS satellite location and the received ray direction. Thanks to this bending angle, doing some data processing, the vapor content, temperature or pressure of the atmosphere can be known. These factors are very important in nowadays meteorological prediction systems. The term occultation comes from the point that the antenna is not directly seeing the signal transmitter, a GPS satellite in this case. An illustration of a radio occultation measurement can be in figure 1.1.

The design that was done in RUAG AB Sweden twenty years ago was used for radio occultation measurements using GPS signals. What was wanted to be done in this Master's thesis was to adapt the old antenna to the Galileo Navigation System (GNS) frequencies of operations.

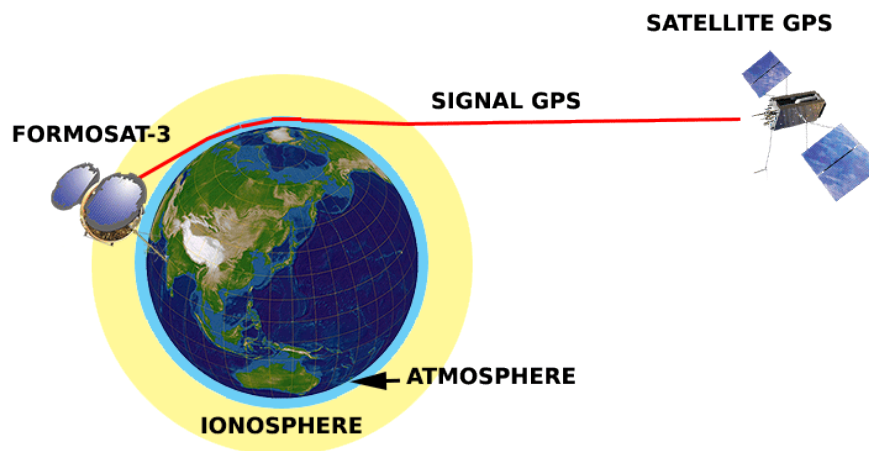


Figure 1.1: Radio occultation working principle

## 1.5 Research Activities on UWB antennas at Chalmers

Antenna Division at Chalmers has been developing wideband antennas for many years. The so-called Eleven antenna has a UWB performance with a nearly constant beamwidth

[5], [6],[7],[8], [9] and [10]. The self-grounded Bowtie antenna [11], [12], [13], [14] and [15] provides a simple solution to ultra-wideband antenna, which finds many applications, such as UWB radar and medical detection. Hat fed reflector antenna is the other one of wideband antenna [16], [17], [18], [19], [20], [21] and [22] which finds the main applications in mini-link and satellite communication systems. The quad-ridge flare horn is a UWB antenna [23], mainly used in radio telescopes because the antenna can only handle low power. However, all these antennas are not planar.

# 2

## Theory

SOME basic theoretical concepts are important to understand the work carried out in this project. This chapter will focus in the antenna element that has been chosen. In order to do so, the different antenna elements studied twenty years ago will be presented and studied. Then, the final choice will be decided from all the options. After that, to finish, the different components of the antenna will be introduced and discussed.

### 2.1 Future Prediction

The future applications of this antenna are actually unknown. Even though it is known that there will be a need of high quality antennas for GNSS applications it is not clear what applications will be. As it was presented previously, the antenna designed twenty years ago was used for Radio Occultation measurements. The antenna that has been designed in this thesis project might also be used for these kind of measurements. What it is known is that in the future there will be a need of array antennas with certain specific features. The applications might be various, for instance, antennas mounted in the international Spatial Station or for some kind of new measurement techniques.

As radio occultation measurements, it is predicted that there will be new measurement applications in the future. One example of such new applications might be the new GEROS-ISS project that they are developing in the ESA [24]. The goal of the project is to combine radio occultation measurements, reflectometry and scatterometry, all mounted in the International Space Station without a need of new satellites. This will help to learn about the sea height, the wave and wind velocity as well as for atmospheric and ionospheric studies, using the techniques mentioned before. GEROS-ISS will be an experiment to demonstrate new ways of observing the earth.

The companies want to be prepared for such new techniques. Due to that, different antenna elements are being studied nowadays. One of these antennas is the one presented

in this project. The goal of this project is to study the antenna and see if it is going to be a suitable antenna element for future applications.

These features will most probably be the following. First, it is going to be important to have a wide antenna beam so the antenna can have a large view. The gain, as always, will be as high as possible. The mechanical properties of the antenna will also be an important characteristic. The physical constructibility will be very important, as well. It is going to be important not only to design an antenna element with good electromagnetic properties but also an antenna element that is easy or at least as easiest as possible to construct. The weight of the antenna will also be an important feature to take into account, as they might be launched in satellites, where the weight is a sensible characteristic.

## 2.2 Different Antenna options

In this section the different antenna element options are going to be presented and compared. This is based on the literature given by reference [25]. In this document the different antennas that were proposed are discussed and compared based on the characteristics presented before.

### 2.2.1 Single Helix Antenna

The first antenna that was proposed was a single helix antenna as the one shown in figure 2.1. It would use one antenna for each of the frequency bands (L1 and L2) With separate antennas for L1 and L2, the pattern can be shaped individually and a gain of about 4dBi can be obtained, over a circular coverage area with 45 degree radius.

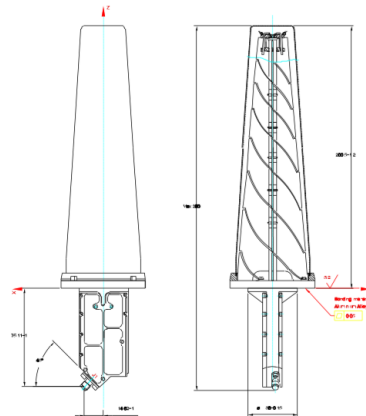


**Figure 2.1:** Single Helix Antenna

Each of these antennas has an approximate mass of about 250g. If we use two antennas, the total mass would be 500g. The antenna in general would be lightweight

which is an advantage. The drawback is the gain which is low for the requirements (4dBi).

### 2.2.2 Linear Array of Helix Antennas

The second antenna that was proposed in the paper was a Linear array of the previously presented helix antennas. The linear helix antenna is shown in figure 2.2. One of the drawbacks of this design was that, due to the space limit, the antenna should work in both L1 and L2 frequencies. The minimum gain pattern of these kind of antennas in earth's limb is 9dB.

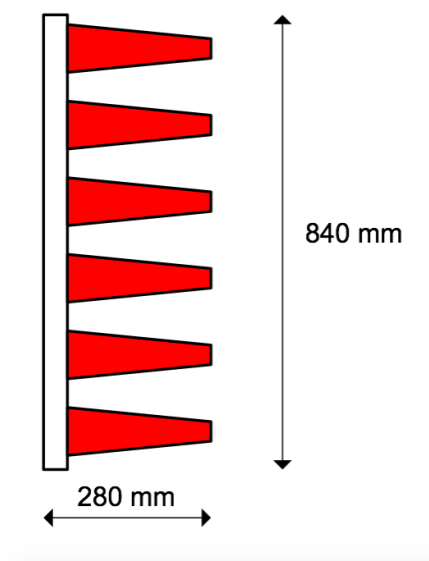


**Figure 2.2:** Linear Array of Helix Antennas

The elements need to be positioned with a spacing that is close to half a wavelength in order to suppress grating lobes in elevation. This gives a coupling between the helices that is quite difficult to predict.

The mass of the helix elements by themselves is about 1.5Kg. With an additional mass of 1.5kg for the structure, the total mass is about 3kg. A more lightweight design of the helix could probably be used to reduce to about 2kg.

### 2.2.3 Array of Large PEC Elements

The third antenna that was studied was an array of large PEC (Patch Excited Cup) array. The array can be seen in the figure 2.3. The patch-excited cup has usually a diameter of 1.0-1.3 wavelengths. The minimum gain along the earth limb for this type of antennas is around 9.0dBi. For these frequencies, the diameter of each element has to be around 240mm. This limits the number of elements to a 2 by 3 array, as shown

in figure 2.3. The mass of each element is around 130g resulting on a total mass of 2kg taking in to account the total structure., which was estimated to be 1.2kg.

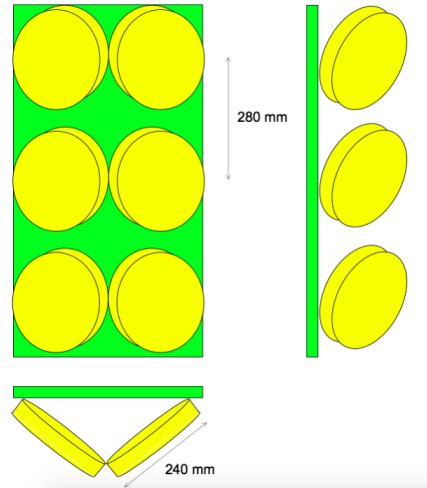


**Figure 2.3:** Array of Large PEC (Patch Excited Cup)

The PEC-s are usually excited by a patch reflector. The main drawback of this is that the excitation sets a resonant mode between the patch and the cup, so it was uncertain if the array could have a dual band operation. This was one of the main reasons why this option was not used.

#### 2.2.4 Printed Resonant Ring Array

The printed resonant ring array was the next antenna design that was studied. The array can be seen in figure 2.4 and as can be seen there it has 18 elements. The maximum allowed antenna dimensions were 840mm in height and 492mm in width. As can be seen in figure 2.4, within these dimensions, the array is a 6 by 3 element array. As it is written in the literature [25], a fourth column and a seventh row could be added, but it gives very little improvement of the beam shaping and it increases the complexity of the feeding network very much. Due to that, the ideal design would be a 6 by 3 array.

The resonant ring array element consists, as the name says, by a resonant printed ring, using suspended skin microstrip technology. In this case, as the antenna element has to work in both L1 and L2, the antenna element needs two resonant rings, one for each of the frequency bands. So, one of the rings needs to be resonant for the L1 frequency band and the other one for the L2 frequency band. These rings are excited through non-resonant slots in a ground plane from separate feed lines for L1 and L2. The structural sandwich is here part of the radiating structure and must comprise only dielectric materials, e.g. a composite with quartz fibres. This gives a thin and mass effective design but there are uncertainties regarding the structural stiffness and thermal stability. The resonant frequency of the rings may also change due to temperature

changes, resulting on a effective dielectric constant variation. The total mass of this array element is estimated to be around 2.0kg.

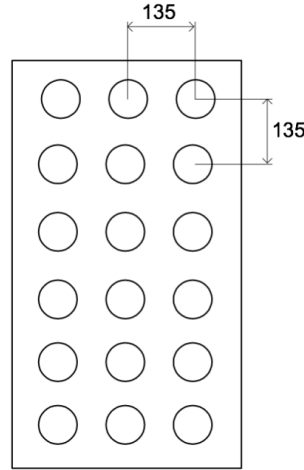


**Figure 2.4:** Printed Resonant Ring Array

The main disadvantages of this structure are that it needs to be protected from Electro Static Discharges by a slightly conducting coating and that all radiating elements must be grounded. This means that several surfaces may be carrying conductive layer which contributes to ohmic losses. A figure of the planar resonant ring array element can be seen in figure 2.5.

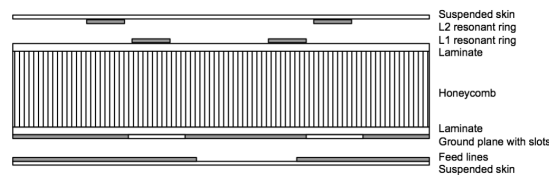


**Figure 2.5:** Printed Resonant Ring Array Element

### 2.2.5 Metalized Resonant Ring Array

An alternative design of the planar array antenna uses a metalized CFRP (Carbon Fiber Reinforced Polimer) sandwich. This structure is excited by slot feeding and supported by dielectric posts as can be seen in figure 2.6. The feeding network, as in the previous antenna, is printed in a suspended skin as in the previous design. In order to obtain an efficient feed from the slots, the elements are embedded in the sandwich. The total mass of the antenna is estimated to about 2.0kg.

The main advantage of this design is that having a front surface that is all metalized, the ESD problems are avoided, and the elements are grounded through carbon loaded dielectric posts.

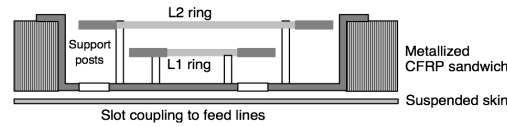


**Figure 2.6:** Metalized Resonant Ring Array using slot feeding

An alternative feed principles with probes is shown in figure 2.7. However, the probe coupling is considered as less advantageous as it increases the couplin between elements and it is sensible to thermal variations.

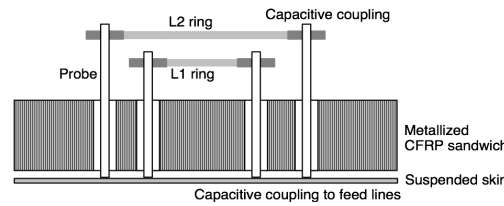


**Figure 2.7:** Metalized Resonant Ring Array using Probe feeding

### 2.2.6 Conclusions

In table 2.1 can be seen a summary of the different properties that were discussed in the previous sections. As can be seen, the resonant ring arrays has much better gain performance, having a gain difference at least as large as 2dB. Due to that, the chosen design was the resonant ring array. Once the design has been chosen, the final choice was between the planar option or the metalized ring option. As it was explained in the previous section, the planar array would need a electro static discharge coating and it was uncertain the response to thermal variations. Due to this reasons the final chosen design would be the metalized resonant ring antenna. In the following sections, the different parts that comprise the antenna will be explained, and the reason why they have been chosen will be explained.

|                                | Gain    | Mass  | X-pol | Struct | ESD |
|--------------------------------|---------|-------|-------|--------|-----|
| Single Helix Antenna           | 4.0dBi  | 0.5kg | OK    | OK     | OK  |
| Array of Helix Antenna         | 9.0dBi  | 2-3kg | ?     | OK     | OK  |
| Array of PEC Elements          | 9.0dBi  | 2kg   | OK    | OK     | OK  |
| Printed Resonant Ring Array    | 11.0dBi | 2kg   | OK    | ?      | ?   |
| Metallized Resonant Ring Array | 11.0dBi | 2kg   | OK    | OK     | OK  |

**Table 2.1:** Summary of different properties

## 2.3 Resonant Ring Array

As it was explained in the previous section, this section will introduce the different parts of the Metalized Ring Antenna.

### 2.3.1 General Antenna Description

The antenna that has been studied in this project is, as said, a Metalized Resonant Ring Antenna, using non-resonant slot feeding. In this section a deep explanation of the antenna is going to be presented. In order to do so, first, the different parts of the antenna are listed below. This will help to understand the antenna studied.

- High Frequency Ring (L1 ring)
- Low Frequency Ring (L2 ring)
- Cavity
- High Frequency Slots
- Low Frequency Slots
- Ground plane
- Feeding network
- Dielectric supporting posts
- Dielectric Screws
- Spacing tool

In the following sections a deeper study of each of the parts is going to be done, in order to understand why they are designed as they are. First a general picture of the metalized ring array can be seen in figure 2.8. This picture is an image from one of the designs done in HFSS. In the image, the different parts of the antenna are shown. First, we can see the cavity. On top of the cavity, the two resonator rings are shown, supported by the dielectric posts. Along with the dielectric posts can be seen the screws that attach the rings to the posts. In the down side of teh antenna, the feeding network can be seen, and below it, the ground plane can be seen.

In the following two pictures (figure 2.9 and 2.10) the top and the bottom of the antenna can be seen, without the transparencies that may lead the reader to confussions. For the bottom side image, the ground plane has been removed, so the feeding network can be seen.

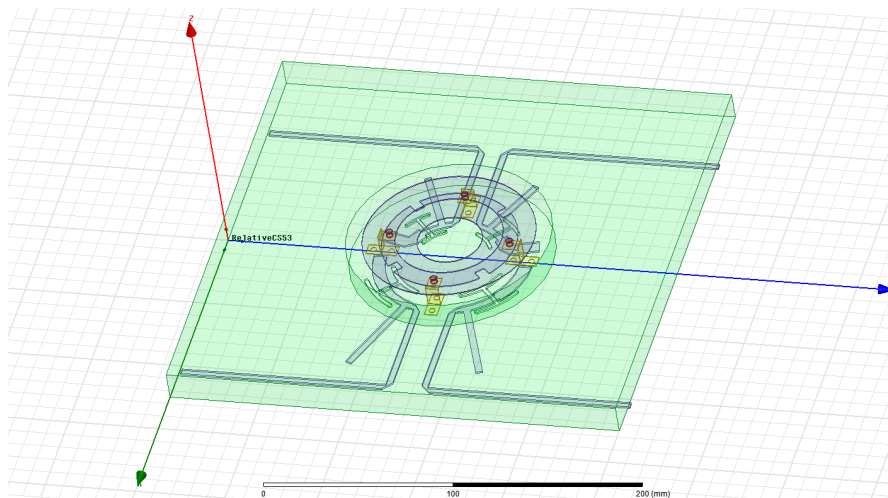


**Figure 2.8:** Metalized resonant ring array design from HFSS

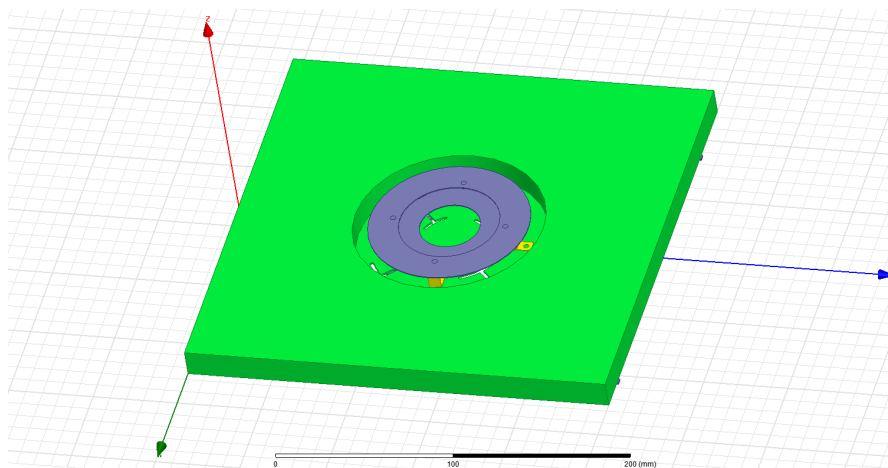


**Figure 2.9:** Top view of metalized resonant ring array design from HFSS

### 2.3.2 Cavity

The cavity is the metallic part of the antenna that supports the resonant rings. The rings are supported in the cavity through the dielectric posts. The cavity contains the slots that feed the resonant rings. The cavity also works as both the top metallic surface of the feeding network, which works like an asymmetric stripline and support for the rings. For simplicity the CFRP sandwich, which was included in the antenna description, is avoided as this is more a concern for the array. Instead, and for more simplicity for the designs and simulations it is set to be metallic. In particular, for the HFSS design the cavity is set to be a perfect electric conductor. A picture of the cavity can be seen in figure 2.11

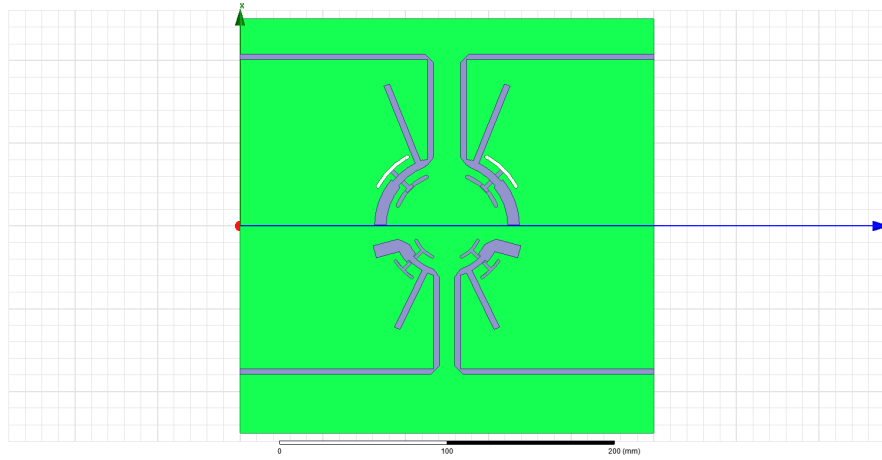


**Figure 2.10:** Bottom view of metalized resonant ring array design from HFSS

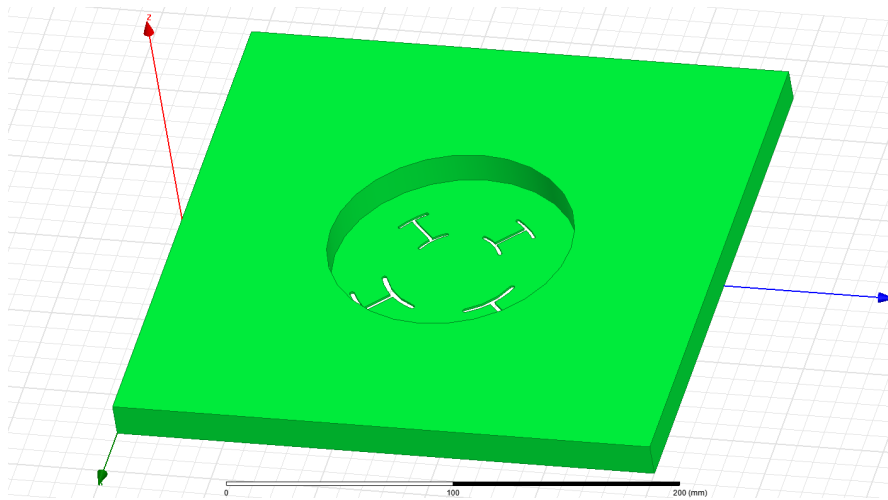


**Figure 2.11:** Image of the cavity

### 2.3.3 Resonator Rings

The ring resonator is the part of the antenna that resonates and radiates the electromagnetic signal. The resonant ring is just a loop antenna. The circumference of the antenna is a wavelength long. That is why there is a resonant mode in the ring. In the case of this antenna, the rings are excited by two slots. The signal from one of the slots is retarded quarter wavelength ( $90^\circ$ ), resulting on a circular polarization. The retardance of the signals produce a circularly varying intensity in the antenna, that is why there is a circular polarization in the antenna. As, it has been said before, depending on the circumference of the ring, the resonant mode of the antenna can be varied. The picture of the high and low frequency ring can be seen in the figures 2.12 and 2.13 respectively.

As can be seen, the high frequency ring has some grooves. This is to improve the

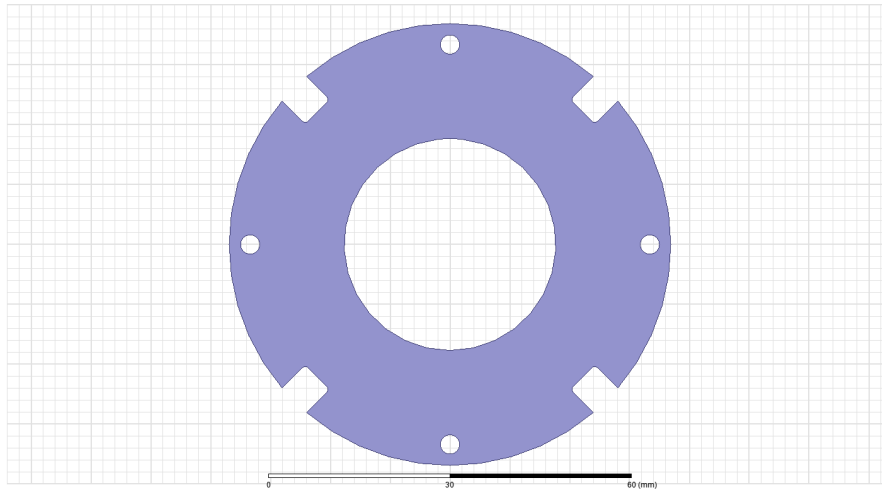


**Figure 2.12:** Image of the high frequency ring

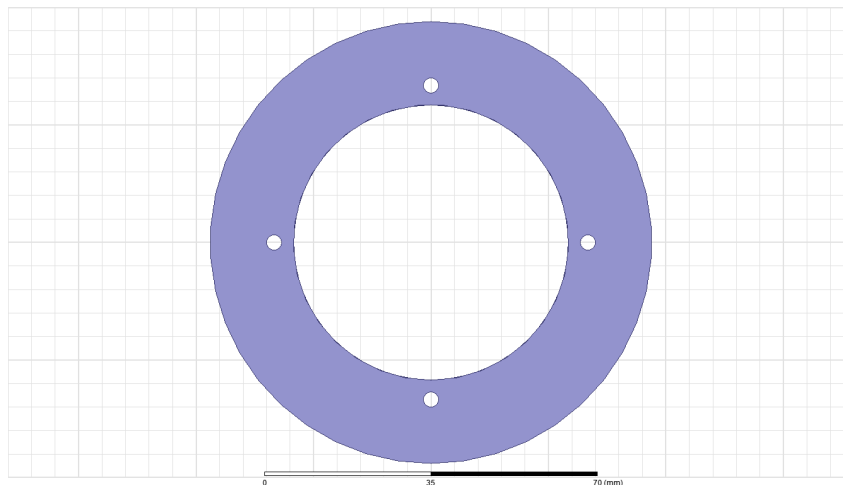


**Figure 2.13:** Image of the low frequency ring

slot feeding to the low frequency antenna, as both rings are placed on top of each other. They also have four holes. Those holes are used to attach the rings to the dielectric posts. They are there only for mechanical reasons.

### 2.3.4 Slots

The slots that are used in this project are H-type slots. The reason of using this slot is that, due to the large frequency of operation, a half wavelength slot cannot be placed in the antenna (space problems). Different slots have been studied during the project. It was clearly seen that the only slots that worked in the required size were the H type slots.

The curved part of the H slots add reactances to the slot input impedance, resulting on a possibility of matching the feeding network to the slot. Thus, the electromagnetic energy is transferred to the resonating rings. In the study we will show how as we shrink the slot it gets more and more difficult to match the feeding network to the slots. The simulator setup and boundary conditions of the design will be left for the next section, where we will focus more on the design and results.

### Slot Study

We start the study from an H-slot, as shown in figure 2.14 and a feeding network composed by a line and a stub.

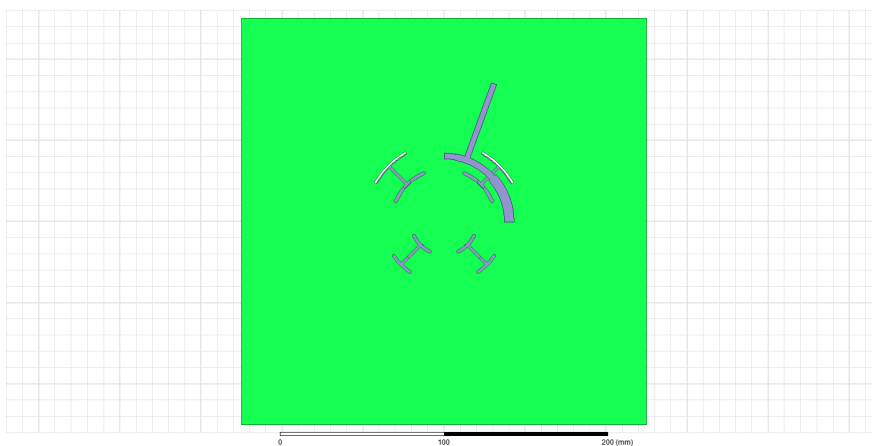


**Figure 2.14:** H slot and feeding network

Having the design in figure 2.14, the results in the smith chart are shown in figure 2.15

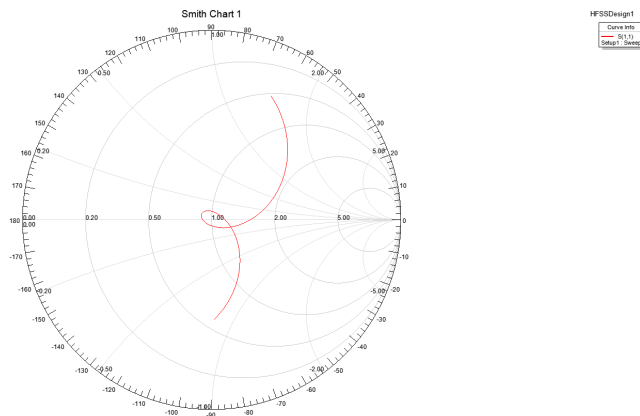


**Figure 2.15:** Matching in the Smith Chart

If a small change is made in the slot size, for example the top curved part of the slot

is shrunk from  $22.5^\circ$  to  $21^\circ$ , and the low curved part from  $15^\circ$  to  $14^\circ$ , the results change. These results can be seen in figure 2.16 and figure 2.17. As can be seen the changes are still not that important, but as we start decreasing the arched parts lengths and the slot start to become a regular slot, the matching starts to be impossible.

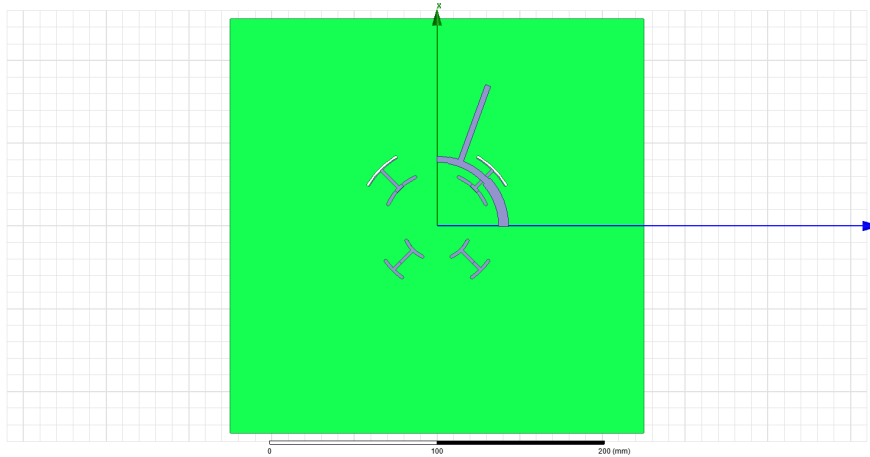


**Figure 2.16:** H slot and feeding network

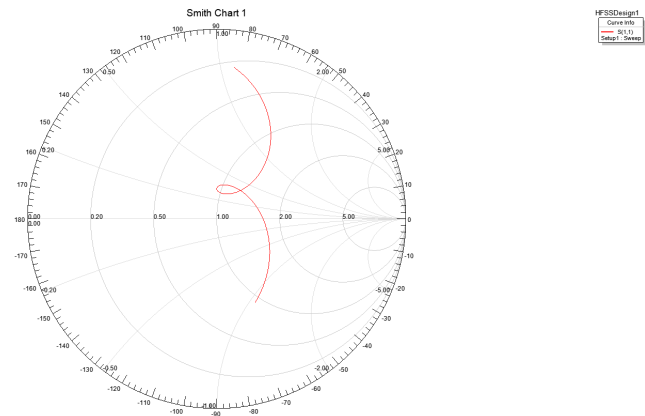


**Figure 2.17:** Matching in the Smith Chart

Once we have this, what we do is to match the feeding back again, playing with the stub and the line length of the feeding network. Using this, a good matching is again obtained, as can be seen in figure 2.18.

Now, the slot is again shrunk. The loop in the smith chart starts to decrease in size and it starts to get farther from the smith chart center. As an example in figure 2.19 and figure 2.20 it can be seen the design when the slots are  $10.5^\circ$  and  $7^\circ$  for the top and bottom arches. As can be seen there is not a loop in the smith chart anymore and the design starts to be very narrowband.

If this steps are followed continuously, the design gets to a stage where the matching

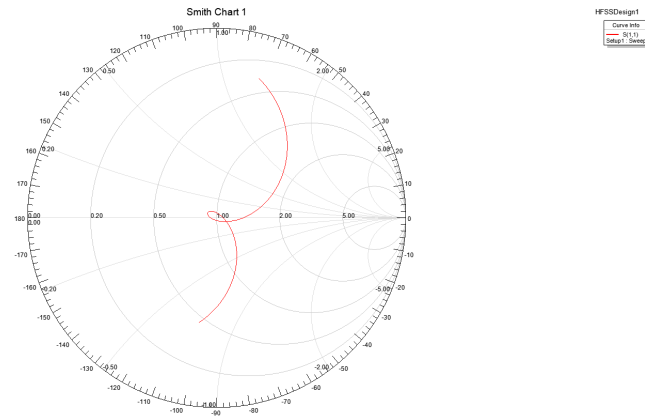


**Figure 2.18:** Matching in the Smith Chart

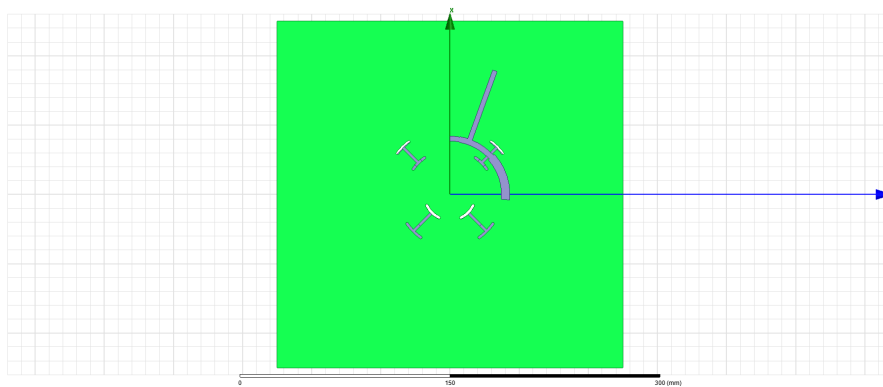


**Figure 2.19:** H slot and feeding network

is impossible. Following this steps, it can be concluded that an H-slot is necessary in the design. This stage is plot in figure 2.21 and ifure 2.22. The figure shows and image when the top and the low archs are  $6^\circ$  and  $4.5^\circ$  respectively.

As an example, this slot could be compared to a Ridge waveguide. The ridge waveguide consists of a rectangular waveguide loaded with conducting ridges on the top and/or bottom walls [26]. A figure of the ridge waveguide can be seen in figure 2.21. This conducting ridges tend to decrease the cutoff frequency of the waveguide. It is the same case as in the slot, where the H-slot tend to decrease the operating frequency of the slot.

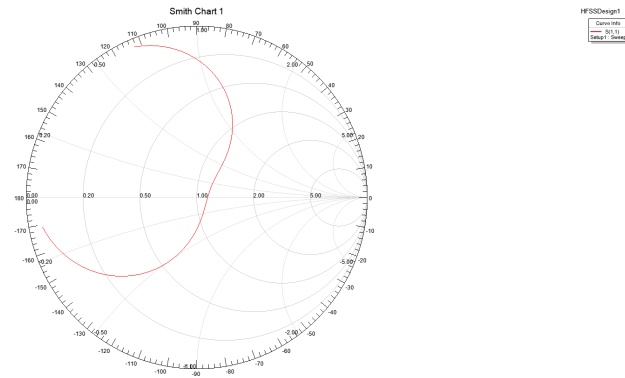


**Figure 2.20:** Matching in the Smith Chart

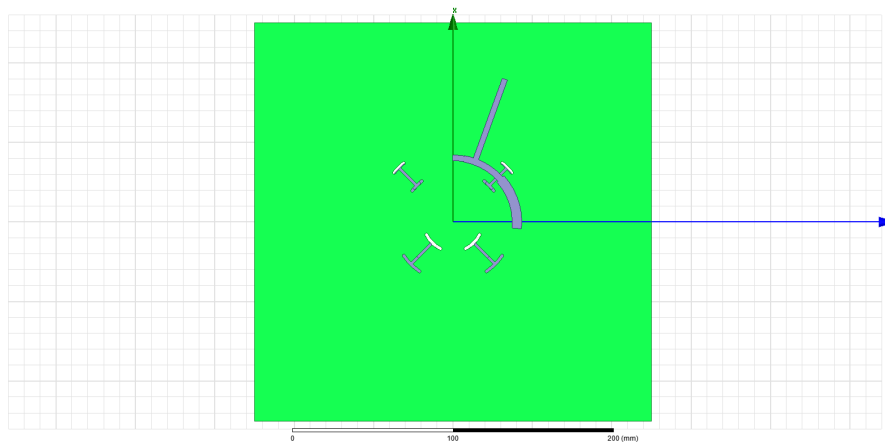


**Figure 2.21:** H slot and feeding network

### 2.3.5 Feeding Network

The feeding network consists on a stripline. This stripline is confined between the cavity and the ground plane. The stripline is a assymetric stripline, as the distance from the cavity is 2mm while the distance from the ground plane is 17mm. The feeding network consists on a typical piece of line-stub mathing network as it could be seen in the previous figures, for instance figure 2.19. The mathing has been designed using HFSS.

### 2.3.6 Ground plane, Screw, Spacing and Posts

In the last section a brief explanation of the rest of the components will be given. The ground plane is the metcalic plate that is mounted 20mm below the cavity. The ground plane is the bottom part of the stripline. The screws used in this design are dielectric screws. The post that supports the plates are also made out of dielectric material, as well as the spacing tool that is used to keep the spacing between the high and low frequency rings.

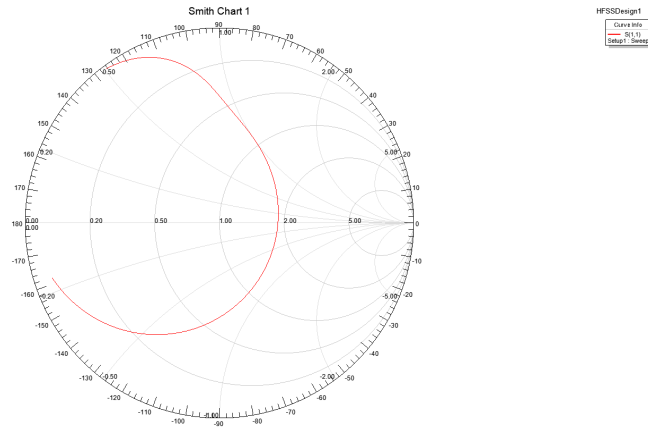
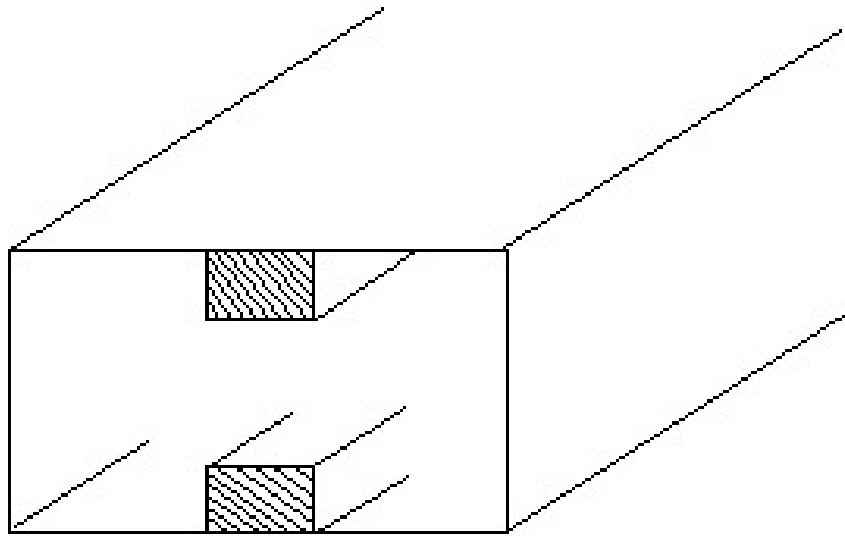


Figure 2.22: Matching in the Smith Chart



## Ridge Waveguide

Figure 2.23: Ridge Waveguide. Figure from: <http://www.rfwireless-world.com/Terminology/ridge-waveguide.html>

# 3

## Redesign Old Antenna

ONE of the challenges at the beginning of the thesis project was the lack of detailed information about the antenna. Some design drawings were available but there was not any drawing regarding the feeding network, which was the most challenging part of the thesis project. Due to that, in the first part of the thesis project the purpose was to design the old antenna again and try to have similar results. This has been done following several steps which are going to be explained in this chapter. The drawings of the different parts of the antenna will not be exposed here, and in case there is interest on them, they are enclosed in the appendix.

### 3.1 High Frequency Slot

The first thing that the design started from was the designing of the excitation of the high frequency slot (L2). At the beginning, only one of the slots was excited. Several ways of exciting the slots were tried. The designing method was a bit difficult as first there were not good results for the coupling. One of the first approaches is shown in figure 3.1, for the high frequency slot. In this design can be seen a straight piece of line combined with a stub, the same architecture as in the final design, but this did not give good results. Along with this design, several other designs were also tried with same results.

After trying several options a design that started to give good results was obtained. This design was composed by a piece of line of different widths combined with a stub. The singularity of this design was that the stub was curved and it followed the slot curvature. A figure of the design can be seen in figure 3.2

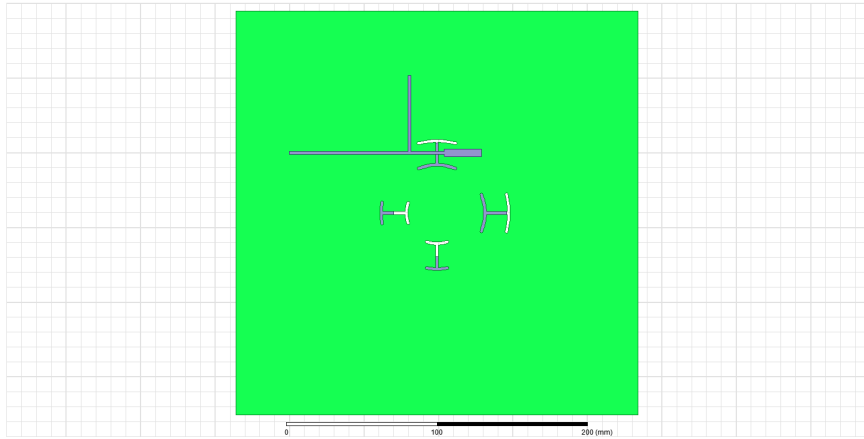


**Figure 3.1:** One of the first design approaches

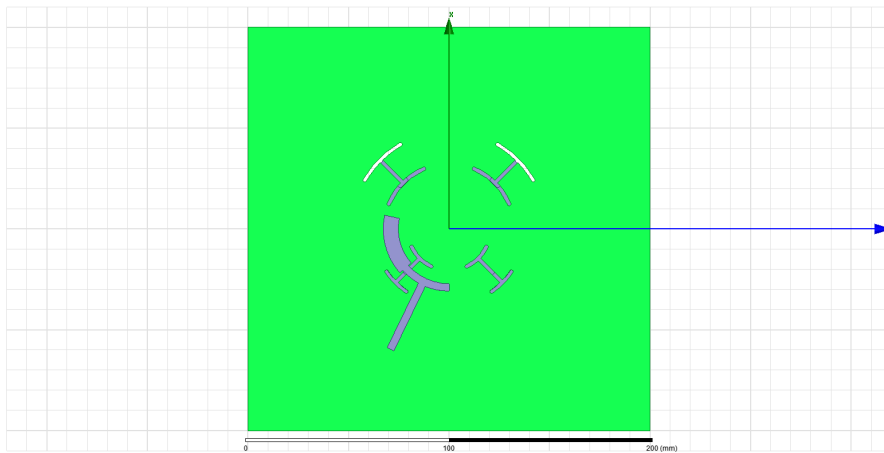


**Figure 3.2:** The design that started to give good results

### 3.1.1 Design Method

In this section, the design method of the feeding network shown in figure 3.2 will be explained. First the overall design is shown in figure 3.3. As can be seen the ground plane is cut in half in the y-axis. This was done to give simplicity to the feeding network, and in order not to have a very complex design from the beginning.

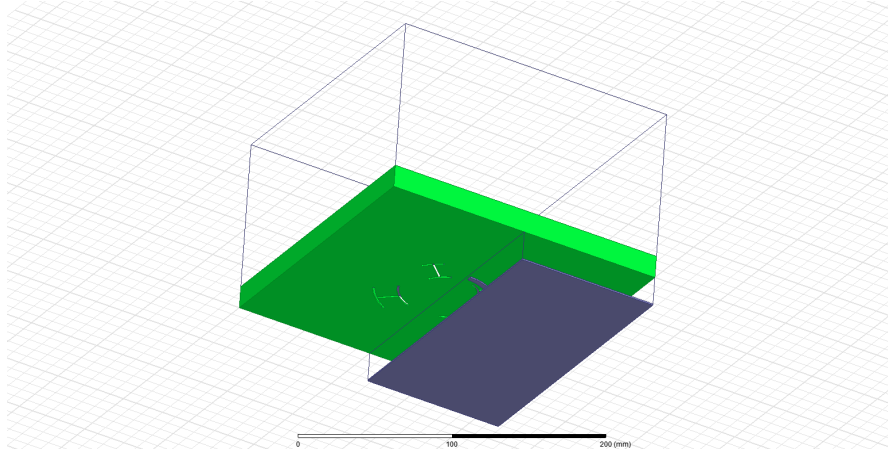


**Figure 3.3:** The overall view of the design

So, in order to begin with the design, the starting point is only a piece of line with different widths, like the one shown in figure 3.4. In order to obtain a good S11 performance, the widths and the lengths of the lines are swiped. Once a fairly good S11 is obtained, for example like in figure 3.5, an stub is added to the line, as in figure 3.2

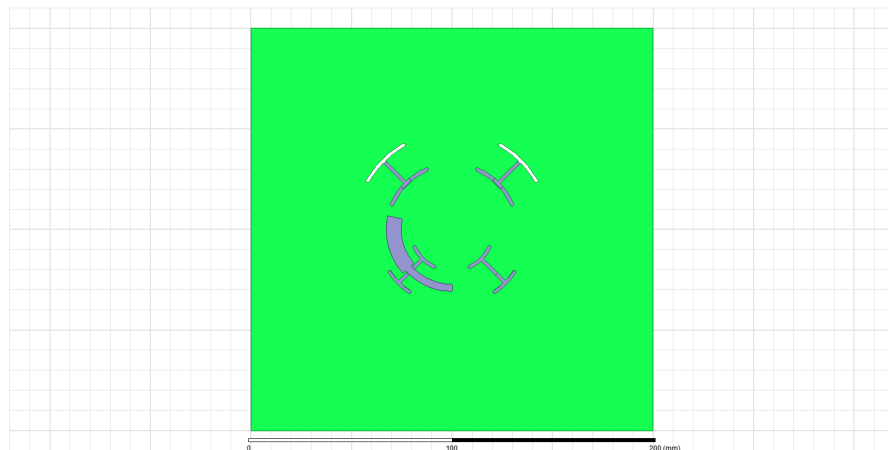


**Figure 3.4:** The first design part of the feeding network

once the stub is added to the figure again the design need to be worked a bit. In this case, the position of the stub is varied in the line, the stub length is also changed and

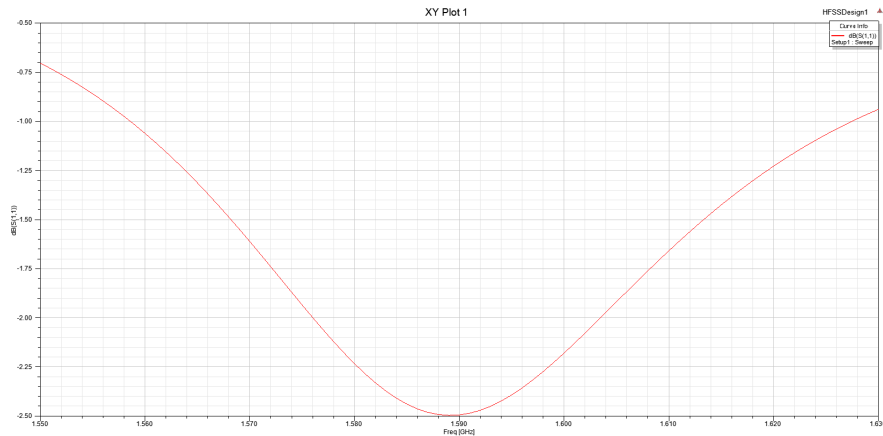


**Figure 3.5:** First stage  $S_{11}$ , when no stub is included

the line length and width again. Working a bit with this design, the  $S_{11}$  shown in figure 3.6, being fairly good.

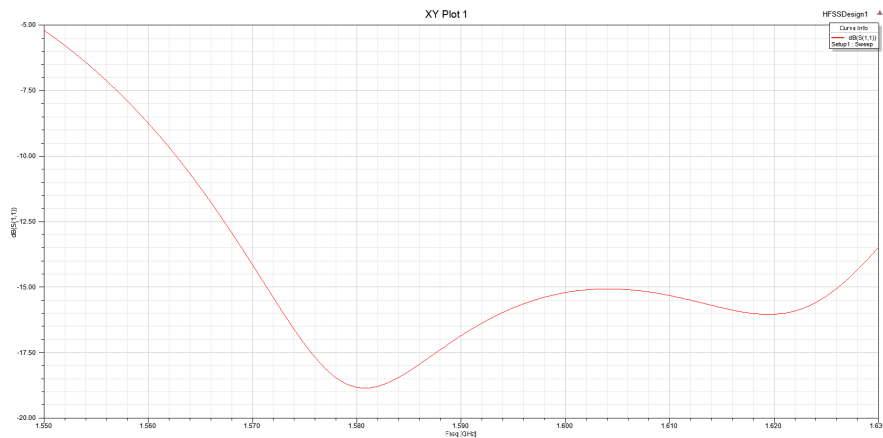


**Figure 3.6:** Final  $S_{11}$

## 3.2 Low Frequency Slot

Once the low frequency slot's feeding network obtained, the next thing to work with is the feeding network of the L2 frequency band's feeding network. The working methodology is exactly the same as for the low frequency band. First, the feeding network is designed using just a piece of line as can be seen in figure 3.7.

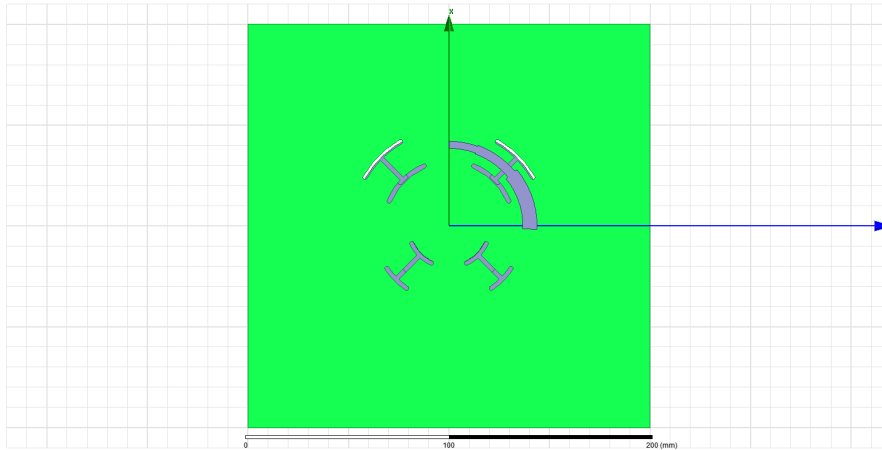


**Figure 3.7:** Low frequency slot first feeding network approach

Once this gives a good  $S_{11}$ , a stub is added to the design and the feeding network is worked again a bit, until a good  $S_{11}$  performance is obtained as in the previous section. A picture of the design with the stub can be seen in figure 3.8 and the resulting  $S_{11}$  can be seen in figure 3.9. With this we obtain a good  $S_{11}$  and we are able to go forward and do the double excitation.

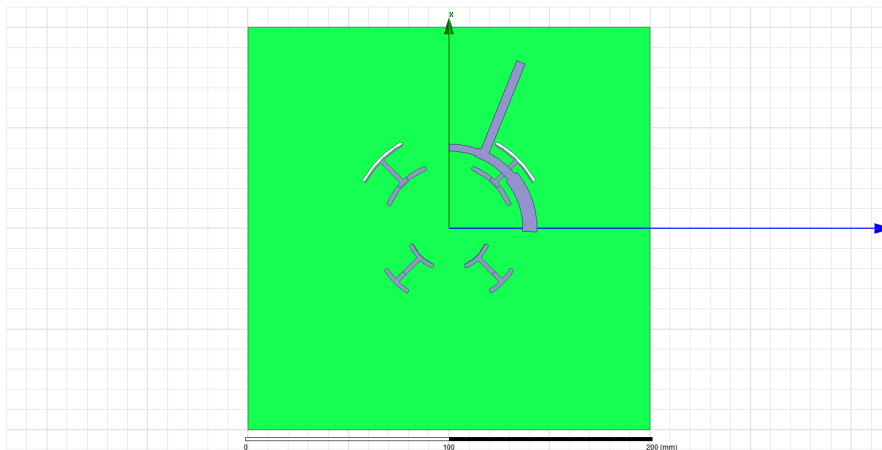


**Figure 3.8:** Low frequency slot first feeding network approach

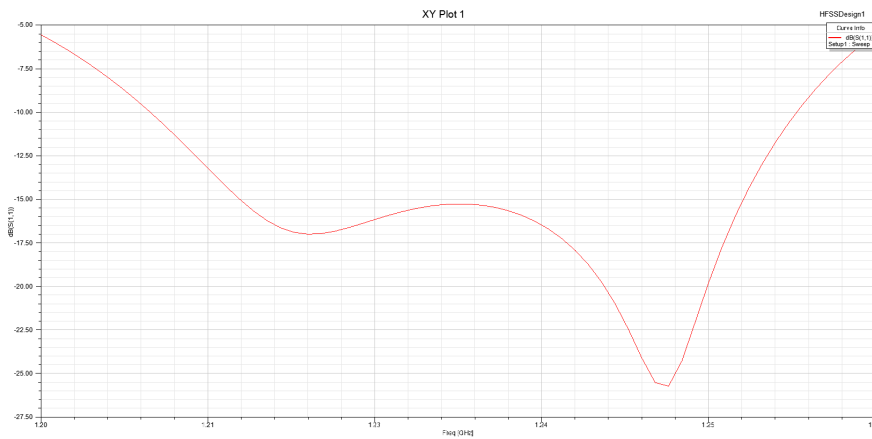


**Figure 3.9:**  $S_{11}$  for large slot

### 3.3 Double Excitation

The step that followed after the single slot feeding was to perform the double slot excitation. In order to do so, the ground plane fully covered the cavity. So, in this case, the ports need to be set in the outer face of the ground plane's vacuum, as can be seen in figure. It can be seen that the new lines are bended as can be seen in figure 3.10. This bending is done using a miter, which is going to be explained in the following subsection.

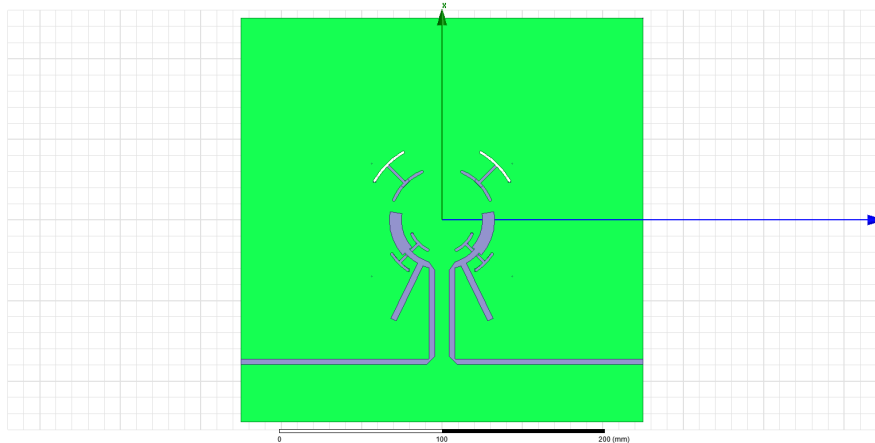
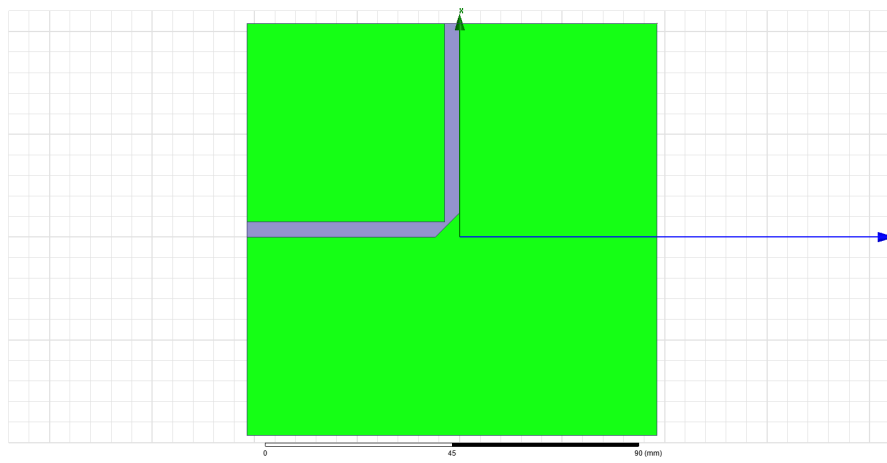


Figure 3.10: Two slot excitation for high frequency

#### 3.3.1 Miter

The miter is the piece of line that it is subtracted in a line in order to bend it. A miter can be seen in figure 3.11. To design a miter is fairly easy having a simulation tool like HFSS. The steps that have been followed in this master thesis are listed below. Following this steps a very good S11 can be obtained for the miter, which is very important to have a better performance of the feeding network.

- Draw the two line junction in a different script
- Subtract the mitter size to the intersection
- Varie the miter size until the best S11 is obtained
- Once this is done, include it in the original design
- Repeat for all the different lines



**Figure 3.11:** An image of the miter

### 3.4 HF double excitation

In this section the high frequency excitation will be explained. An image of the matching network is shown in figure 3.12. For this design, the previous design for only one slot have been used combining with a miter.

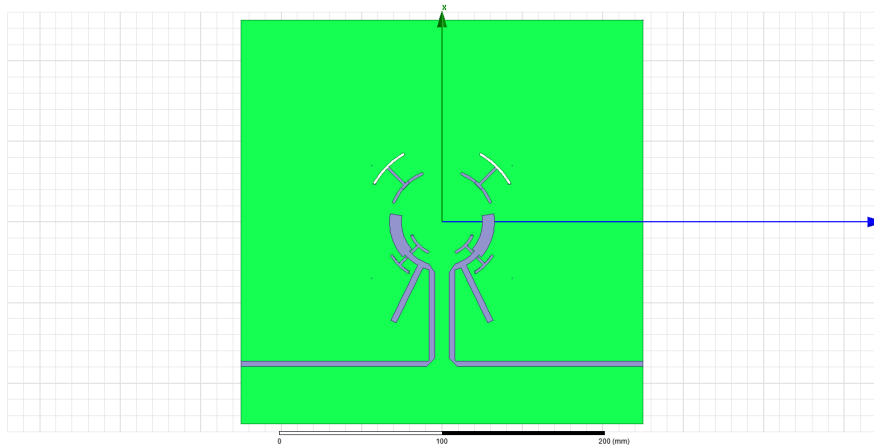


**Figure 3.12:** Two slot excitation for high frequency

The design of figure 3.12 has been obtained using varying the design for only one slot a bit. The key has been to play with the line length, the stub position and their respective widths. Following these steps, the obtained S11 can be seen in figure 3.13. The bandwidth of the L1 frequency band lies between 1565-1614MHz. As can be seen in figure 3.13, the matching is very good for this frequency. The plot of the Smith Chart can also be seen in figure 3.14.

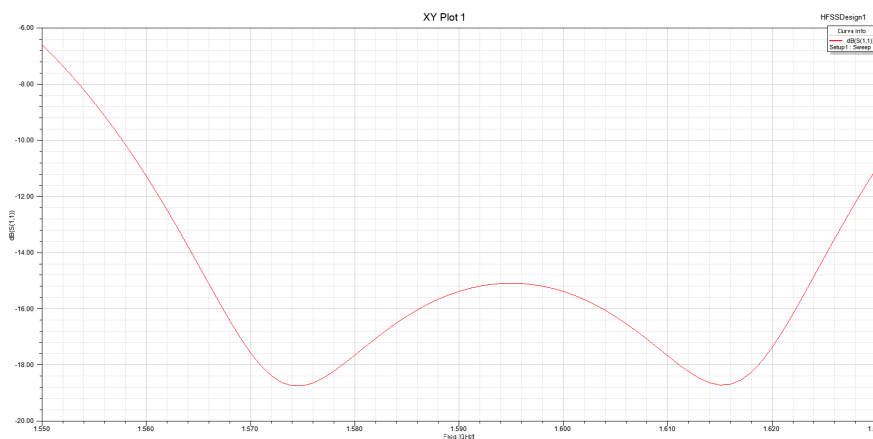


**Figure 3.13:** Reflection coefficient for the high frequency slots feeding network

With the matching above, the radiation patterns for the antenna can be seen in figure 3.15 and figure 3.16. The first one is for the co-polar radiation pattern and the second

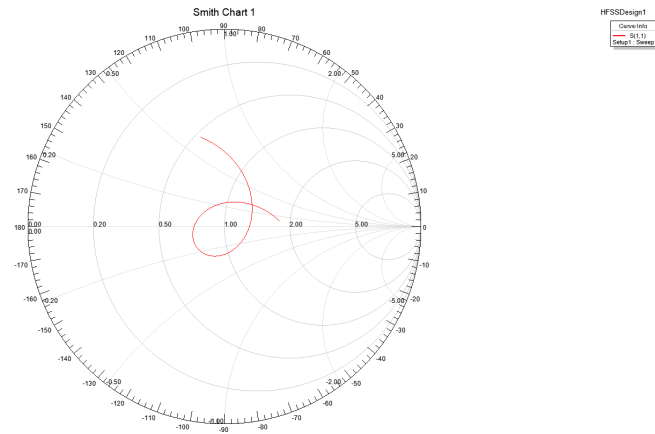


Figure 3.14: Reflection coefficient for the high frequency slots feeding network, represented in the Smith Chart

one is for the cross-polar radiation patter.

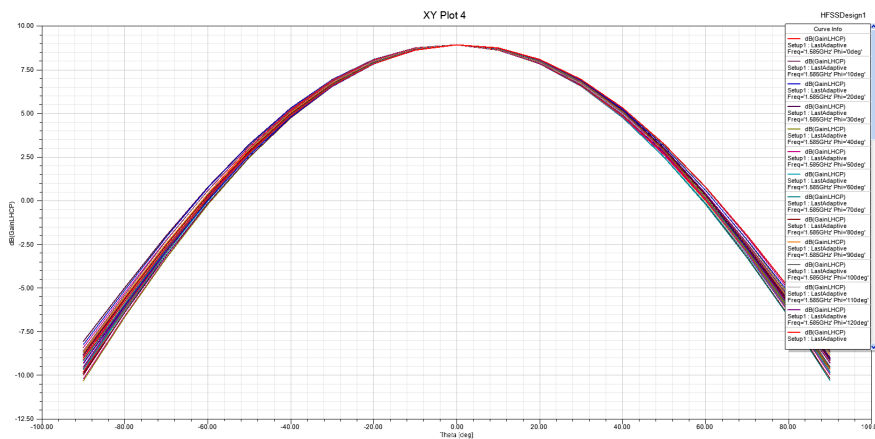


Figure 3.15: Co-polar radiation patter

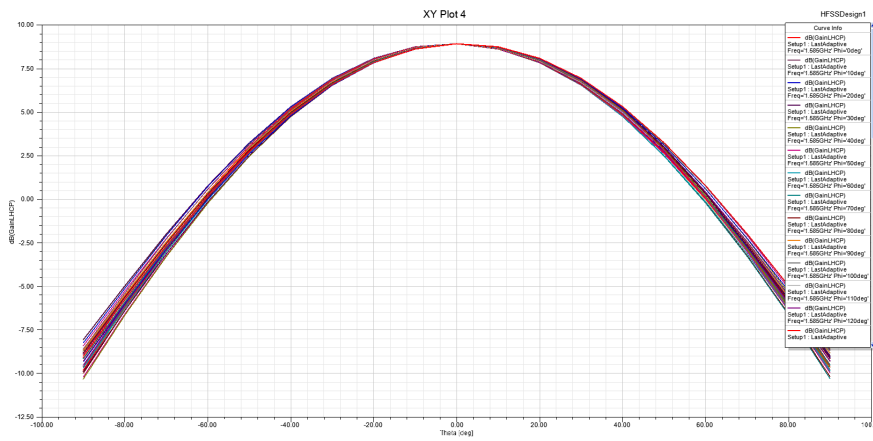
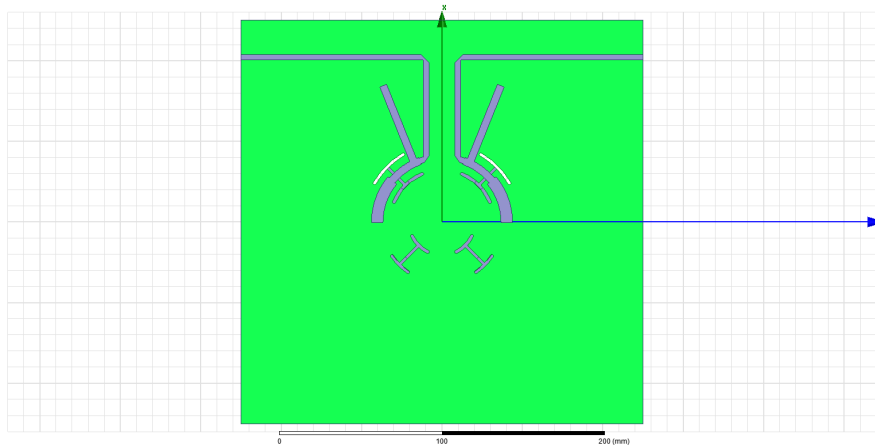


Figure 3.16: Cross-polar radiation pattern

### 3.5 LF double excitation

For the low frequency (L2) the design method has been the same as for high frequency (L2). The design for a unique slot has been used as an starting point, and some changes has been done in order to obtain the best S11. A miter has also been used to bend the lines. The plot of the feeding network for the lower frequency can be seen in figure 3.17.



**Figure 3.17:** Two slot excitation for low frequency

Having this design, the reflection coefficient of the design can be seen in figure 3.18 and the smith chart representation can be seen in figure 3.19. As before, the co-polar and cross-polar radiation pattern of this design can be seen in figure 3.20 and figure 3.21.

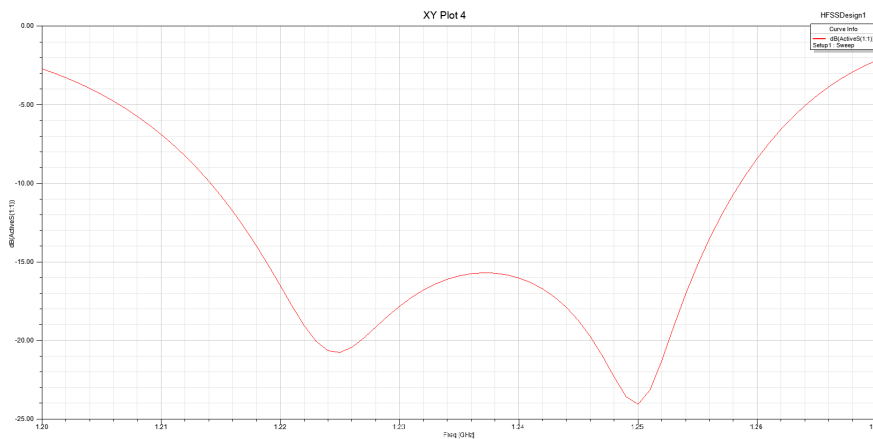


**Figure 3.18:** Reflection coefficient for the low frequency slots feeding network

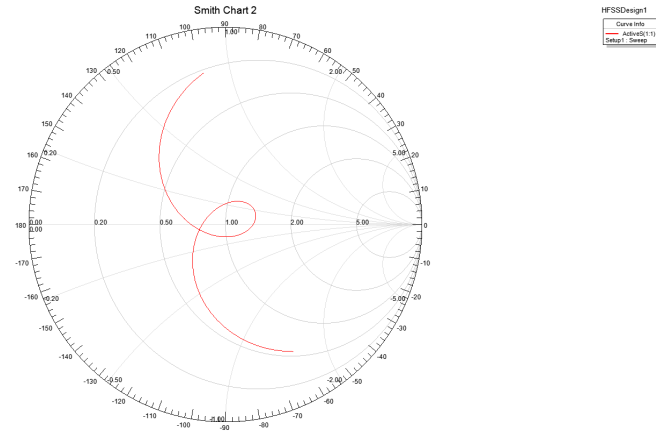


Figure 3.19: Reflection coefficient for the low frequency slots feeding network, represented in the Smith Chart

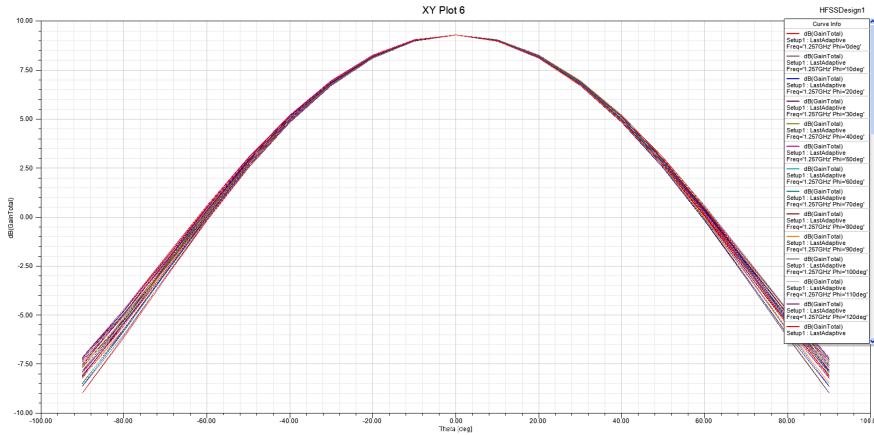


Figure 3.20: Co-polar radiation pattern

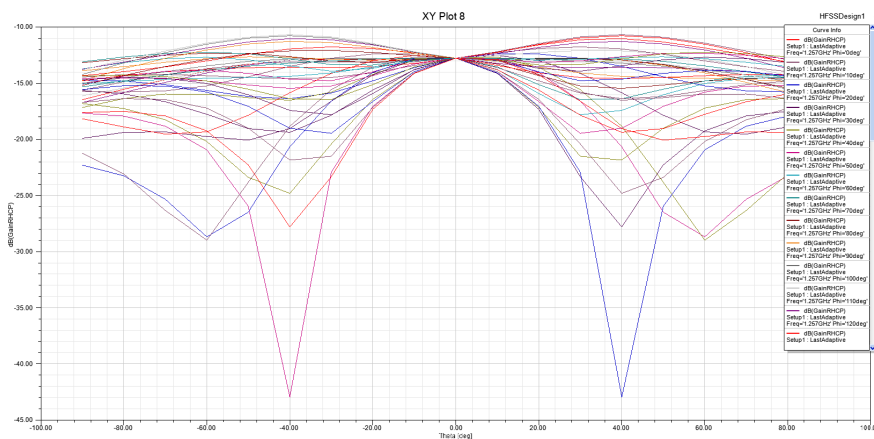


Figure 3.21: Cross-polar radiation pattern

### 3.6 Everything together

The last part of the redesign process is to put everything together. So, in this part all the feeding networks designed before are put together. The complete design can be seen in figure 3.22. As can be seen, in order to fit the lines in the space, the high frequency line has been bent using a miter. This allows the design to fit in space. With this design, the results are plotted in figures from 3.23 to figure 3.34. The first pictures are the pictures for the high frequency and the second ones are for the low frequency.

This gives us good results for the frequency band of interest. This results could probably be improved but what was decided was not to lost time on improving small things in the design and instead to continue the design by trying to increase the bandwidth of the ring so it could be possible to include a third frequency band, the L5 frequency band.

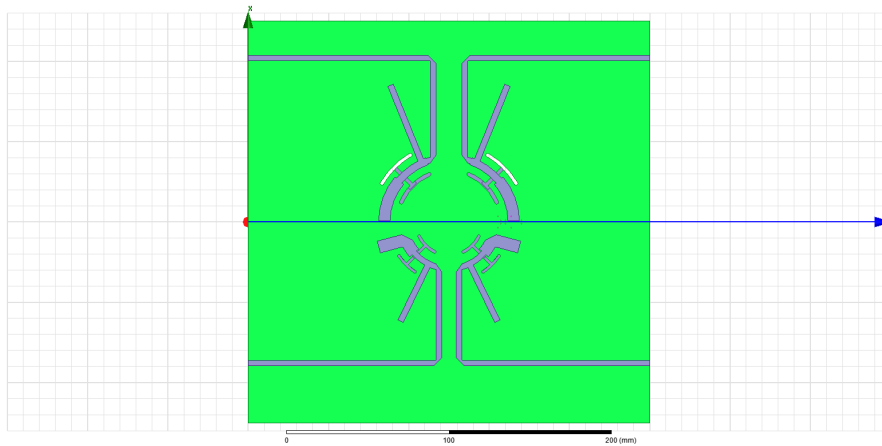


Figure 3.22: Final design complete

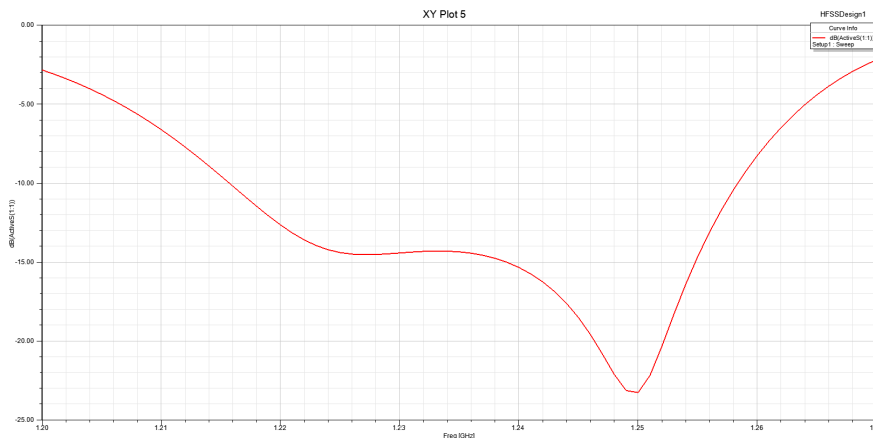


Figure 3.23: S11 port 1, L2 frequency band

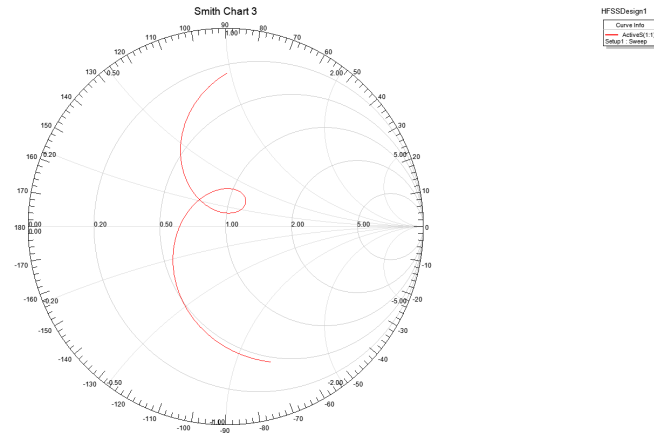


Figure 3.24: Smith Chart port 1, L2 frequency band

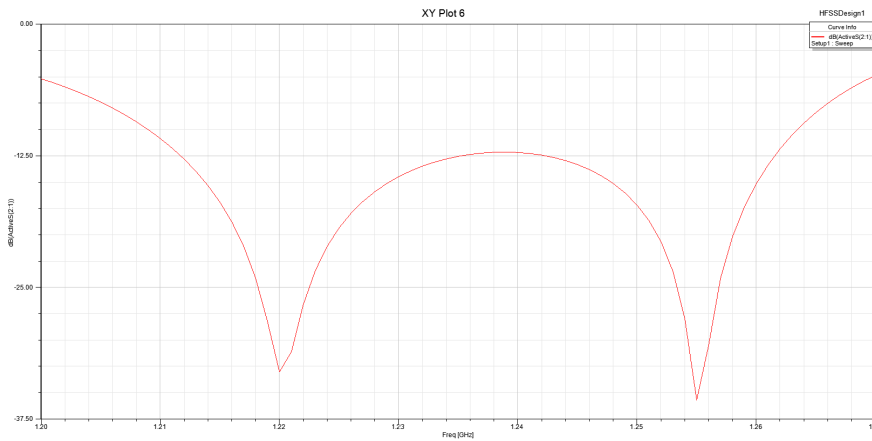


Figure 3.25: S11 port 2, L2 frequency band

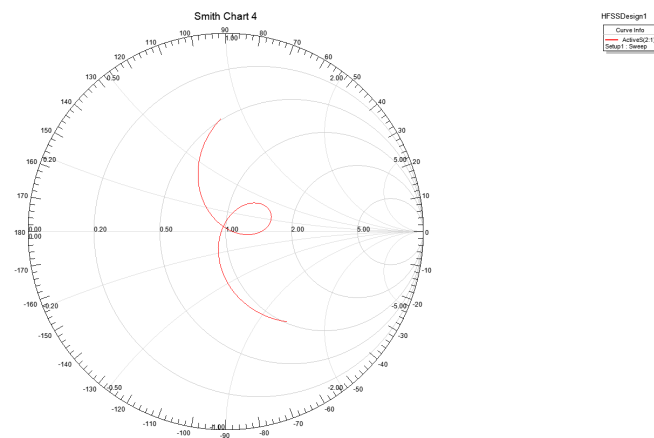


Figure 3.26: Smith Chart port 2, L2 frequency band

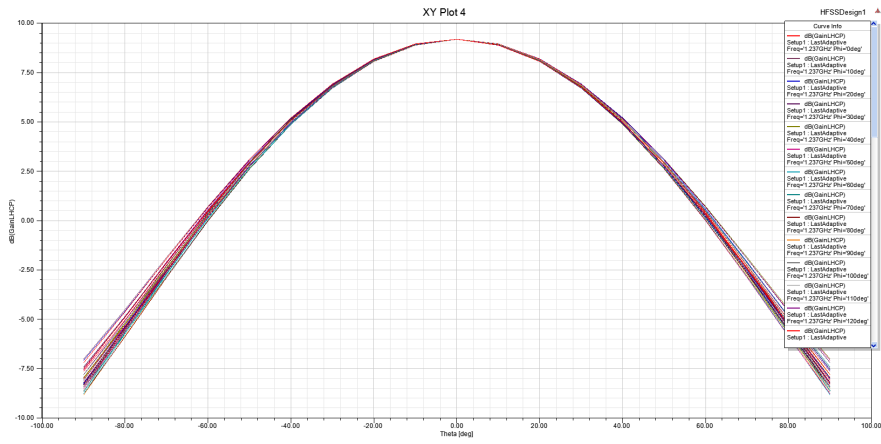


Figure 3.27: Co-polar radiation pattern

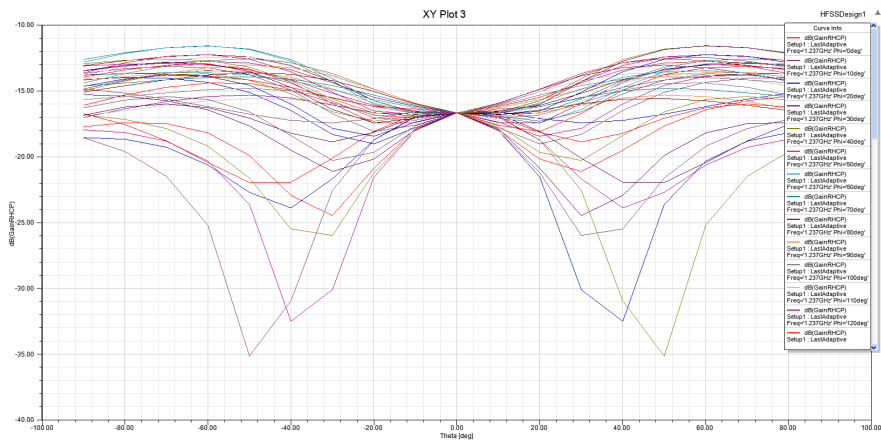


Figure 3.28: Cross-polar radiation pattern

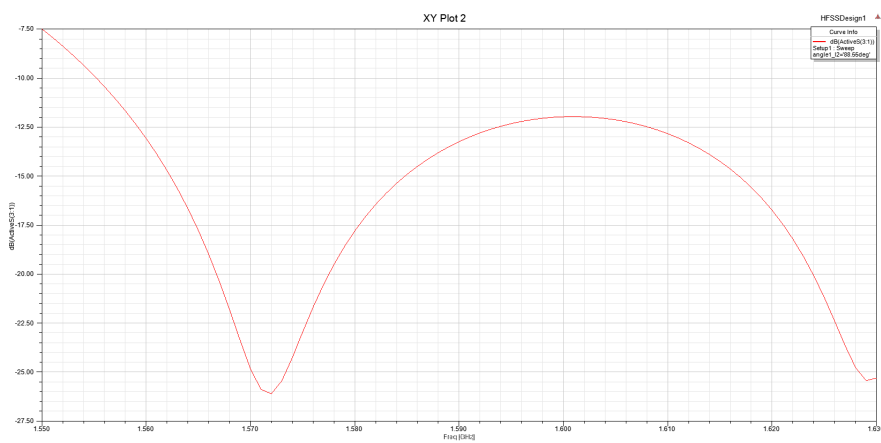


Figure 3.29: S11 port 3, L2 frequency band

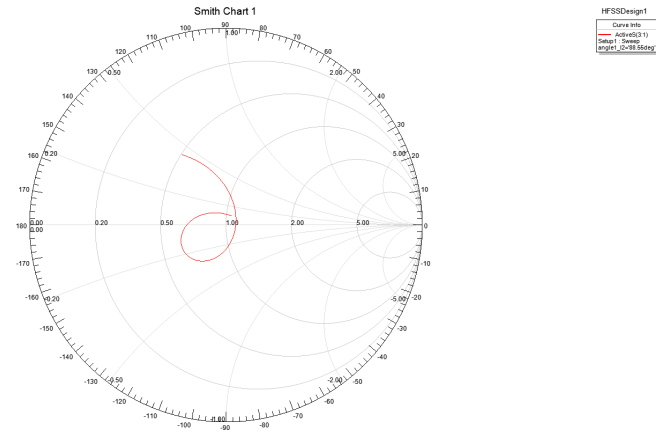


Figure 3.30: Smith Chart port 3, L2 frequency band

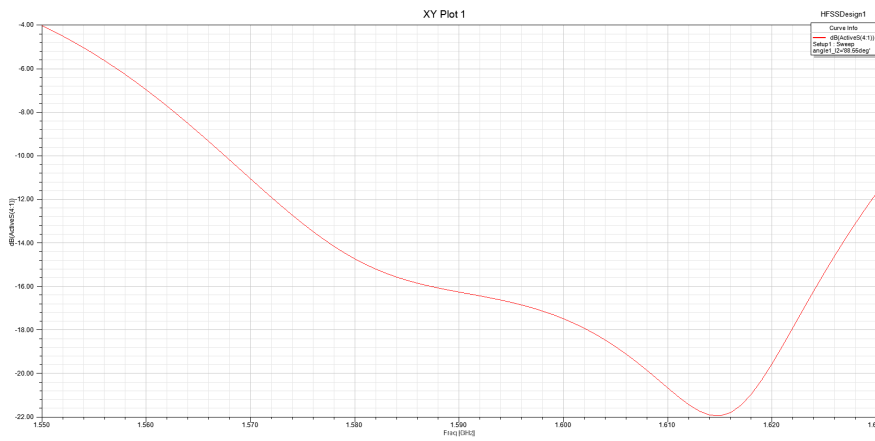


Figure 3.31: S11 port 4, L2 frequency band

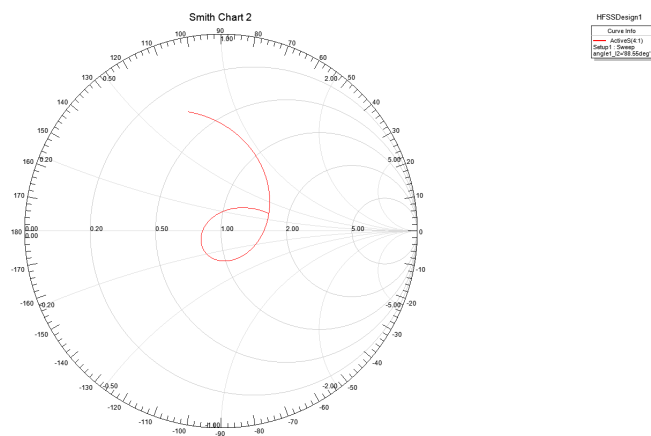


Figure 3.32: Smith Chart port 4, L2 frequency band

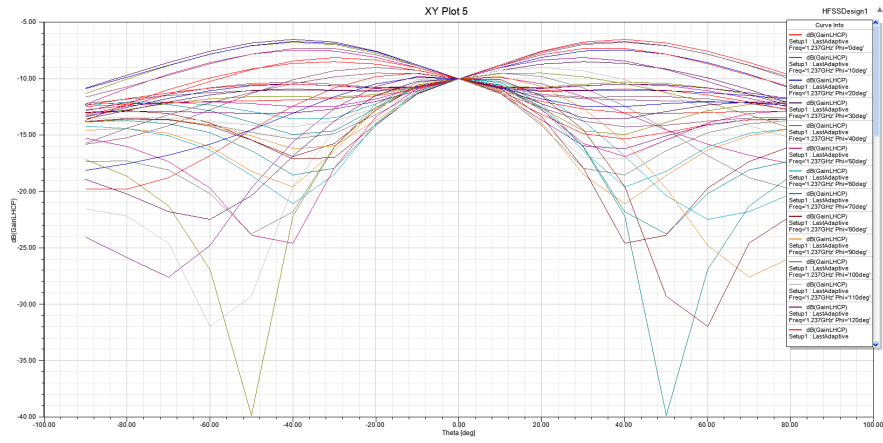


Figure 3.33: Co-polar radiation pattern

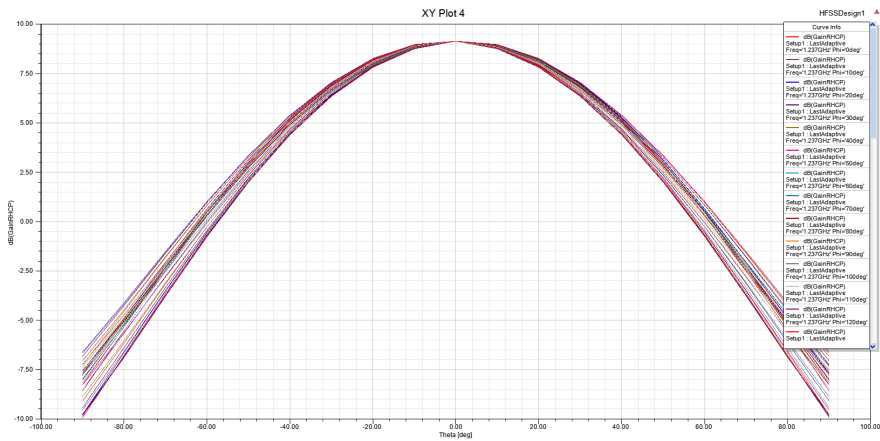


Figure 3.34: Cross-polar radiation pattern

# 4

## Improve the bandwidth

THE next part that followed the master thesis was to try to improve the bandwidth of the antenna. The purpose of the thesis was to see if the antenna could support another frequency band. The additional frequency band was the L5 frequency band. The mentioned frequency band is centered around 1176.45MHz, very close to the L2 frequency band which is centered around 1227.6MHz. Several possibilities were studied in order to achieve the goal of having an antenna working on the three different bands. The first trial was using a double stub based feeding network. This method did not succeed, as it was impossible to increase the bandwidth of the L2 band. After this first trial, a patch system was tried, having the same results as in the previous one. The next design that was tried was to include a third ring to the design. The problem with the third ring was that there was too much coupling between the L2 ring and the mentioned new L5 ring, being impossible to have a successful design. With this design together, a different method was performed to see the inherent bandwidth of the rings and the effects between each of the rings. Lately, a wider ring method was tried, in order to have two feeding networks for the same ring but at different frequency bands. This was also impossible to achieve as the ring by itself was the component that set the working frequency. So, the purpose of this chapter will be to show all the different designs tried to increase the bandwidth, based on all the results obtained. With this results the impossibility to increase the bandwidth will be shown.

### 4.1 Double Stub Matching

The first thing that was tried in order to increase the bandwidth of the design was to include the double stub matching and see if an increase in bandwidth was possible. The design was based on the previous design. In this case it was only tried to increase the bandwidth of the L2 feeding.

In figure 4.1 can be seen the design that was started from and in figures 4.2 and 4.3

can be seen the reflection coefficients of the design. Starting from this design a double stub matching was added and see if the bandwidth of the design was improve.

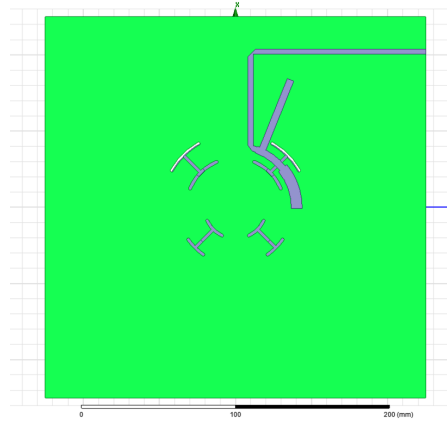


Figure 4.1: Double stub matching, the starting design

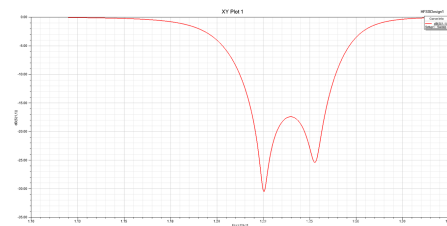


Figure 4.2: S11 double stub matching

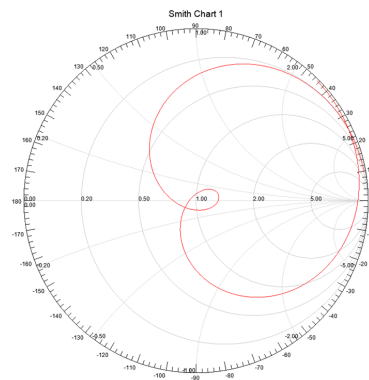


Figure 4.3: reflection coefficient in the smith chart for the double stub matching method

The stub was added step by step. So first a small piece of stub was added at around quarter of wavelength distance from the previous design. This design can be seen in figure 4.4, and the reflection coefficient can be seen in figure 4.5 and 4.6.

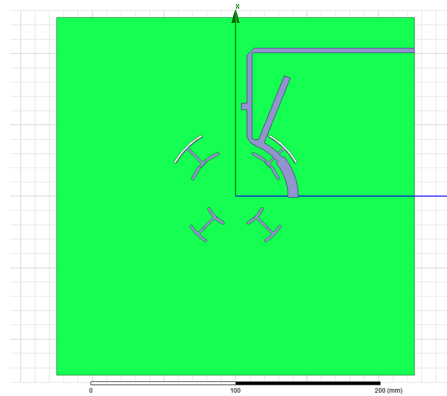


Figure 4.4: Double stub matching

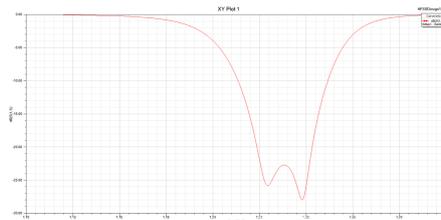


Figure 4.5: S11 double stub matching

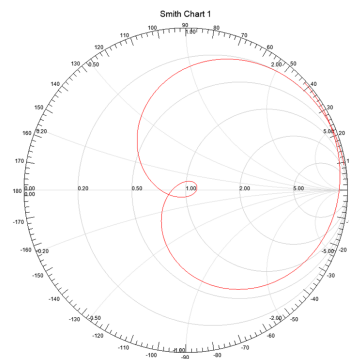


Figure 4.6: reflection coefficient in the smith chart for the double stub matching method

Now, as the reflection coefficient did not change very much, the stub was made longer. This design can be seen in figure 4.7, and the reflection coefficient can be seen in figure 4.8 and 4.9.

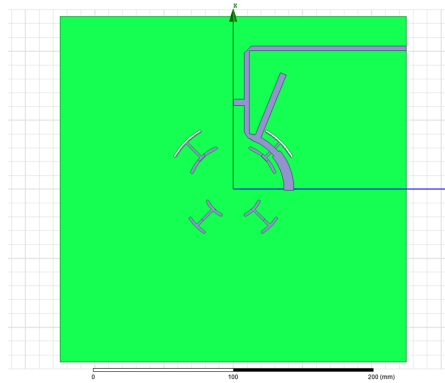


Figure 4.7: Double stub matching

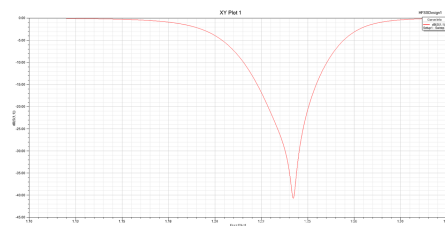


Figure 4.8: S11 double stub matching

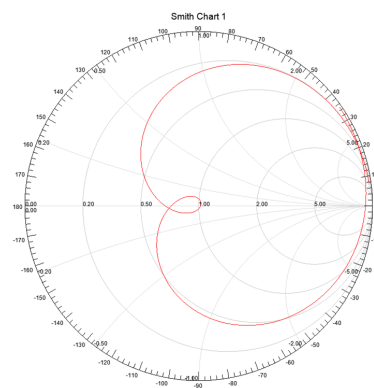
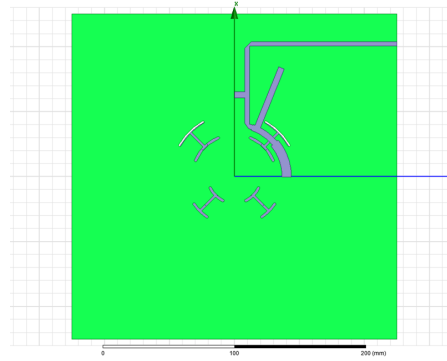


Figure 4.9: reflection coefficient in the smith chart for the double stub matching method

Now, as can be seen, the reflection coefficient has changed a bit, so what was done now is to adjust the stub and the line in order to have a proper reflection coefficient. So, what was done now was to adjust the stub and the line so that we have the loop again in

the center of the smith chart. This design can be seen in figure 4.10, and the reflection coefficient can be seen in figure 4.11 and 4.12.



**Figure 4.10:** Double stub matching

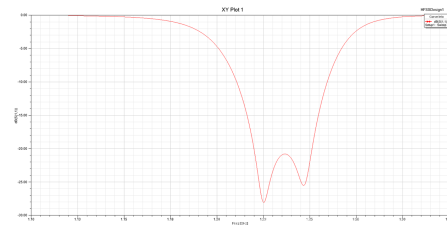


**Figure 4.11:** S11 double stub matching

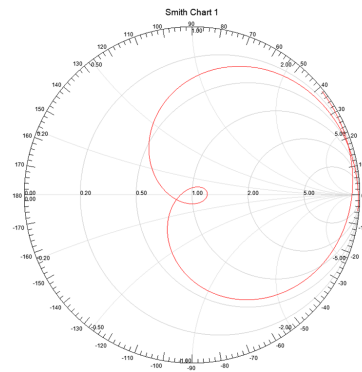


**Figure 4.12:** reflection coefficient in the smith chart for the double stub matching method

So, following this process, a stub could be added to the design. All the design process will be avoided as it is just following the same steps as the ones explained above. What it is going to be shown is the last design that was obtained following this steps. This design can be seen in figure 4.10, and the reflection coefficient can be seen in figure 4.11 and 4.12. In this case the length of the stub is 52.8mm.

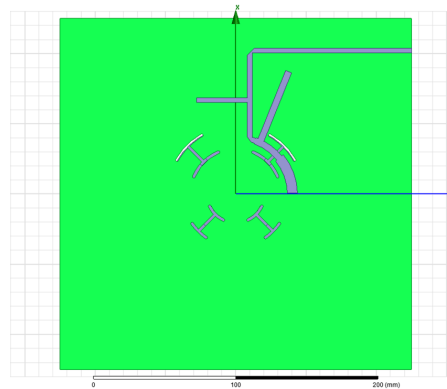


**Figure 4.13:** Double stub matching

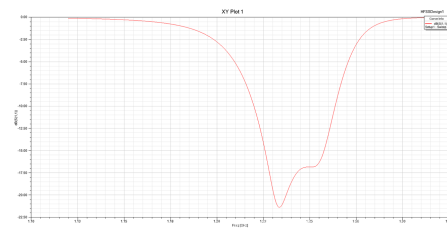


**Figure 4.14:** S11 double stub matching

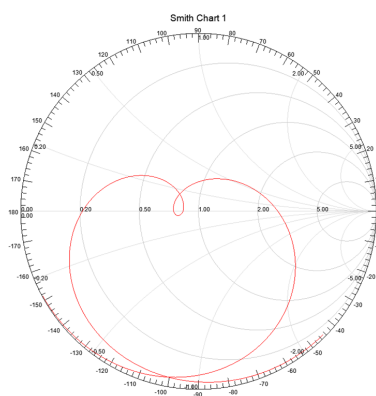


**Figure 4.15:** reflection coefficient in the smith chart for the double stub matching method

As can be seen, even though a double stub matching was added to the design, there was no improvement in the design's bandwidth. It was concluded that with a double stub matching it was impossible to achieve a bandwidth improvement so other designs were tried in order to improve the bandwidth of the design.

## 4.2 Adding a patch

The second proposed solution, after the double stub matching, was using a patch on top of the slot. This idea came from the method that it is used in patch antennas to increase the bandwidth. In such antennas, if a patch is placed on top of another patch, at a certain distance, the bandwidth of the first patch without any modifications is increased. So, the proposed solution after the double stub matching was to try to increase the bandwidth of either the slot or the ring by placing a patch on top of it. As before, the design was started from the old design, having the characteristics shown in figures 4.16, 4.17 and 4.18.

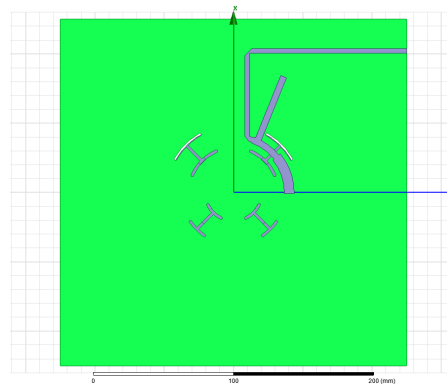


**Figure 4.16:** The starting point design

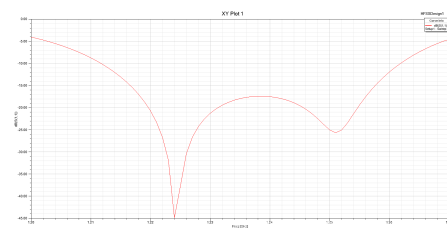


**Figure 4.17:** The starting point design

Having this design, a patch was added to the slot. The design can be seen in figure 4.19. The rings are taken out of the picture in order to be able to see the patch. Making this change, the results for the reflection coefficient can be seen in figure 4.20 and figure 4.21.

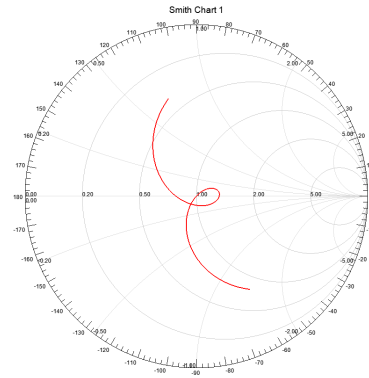


**Figure 4.18:** The starting point design

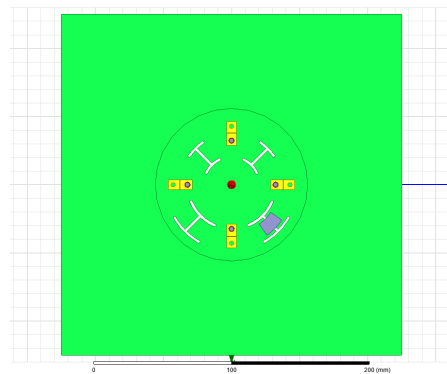


**Figure 4.19:** The patch on top of the slot. The rings are not shown in the figure as it could not be possible to see the patch otherwise

After adding the patch, it can be seen that the resonant loop was moved a bit in the Smith chart. Modifying the stub length and the lines from the feeding network, it was possible to match the resonant loop in the center of the Smith chart again. Such a result can be seen in figures 4.22 and 4.23.

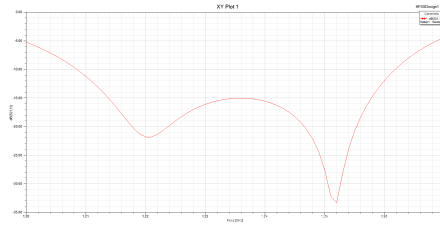


Figure 4.20: The reflection coefficient after the S11 is added to the design

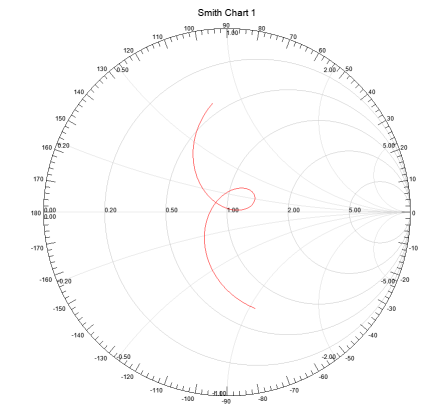


Figure 4.21: The reflection coefficient plot in the Smith Chart

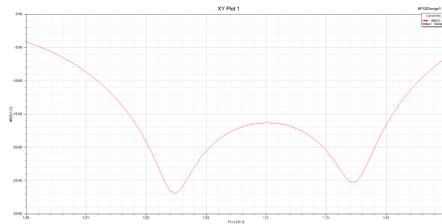


Figure 4.22: The reflection coefficient after the S11 is added to the design

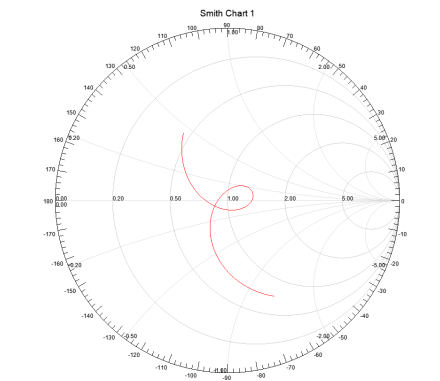
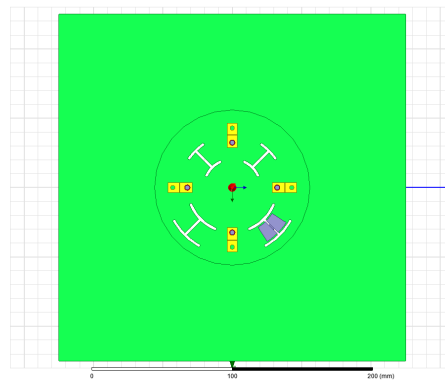
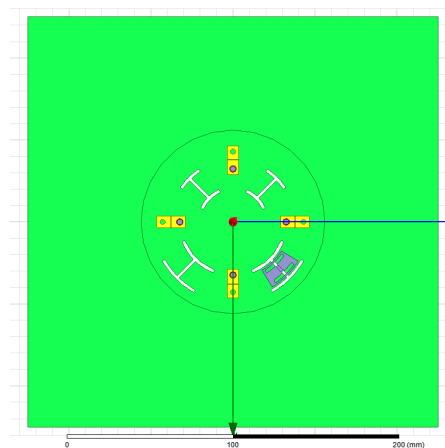


Figure 4.23: The reflection coefficient plot in the Smith Chart

As, it can be seen in the figures, the bandwidth is not really increased after adding the patch. Several other patch dimensions and designs were also tried but their deep study is going to be avoided in this report as they did not give any good final results and would only add useless information to the report. T Even though, in a couple of images can be seen the different patches that were tried during the design period. In figure 4.24 can be seen a design that has a patch cut in half, that has like a slot in the middle. In the second figure, figure 4.25, a patch with a slot can be seen. This did not give any good results either so it was decided to continue trying other solutions and give up with the patch.



**Figure 4.24:** A patch cut in half having a groove in the middle



**Figure 4.25:** A patch with a slot

### 4.3 Adding a third ring

After the first two proposed solutions, in the third trial instead of trying to increase the bandwidth of the L2 ring, a third ring was added for the L5 frequency band. The dimensions of this ring were so that it was resonant at the L5 frequency. These dimensions were the following,

- $R_{out}=50.9\text{mm}$
- $R_{in}=29.3\text{mm}$

So, first what was tried was to see how adding the ring affected the previous design. So, what was done first was to add a third ring to the previous design. First the design started as before from the old design done previously. First it was tried only for the design when the low frequency is excited. This design can be seen in figure 4.26 and figure 4.27. Afterwards it was also seen for the design were only the high frequency was excited and finally the design were both frequency bands were excited.

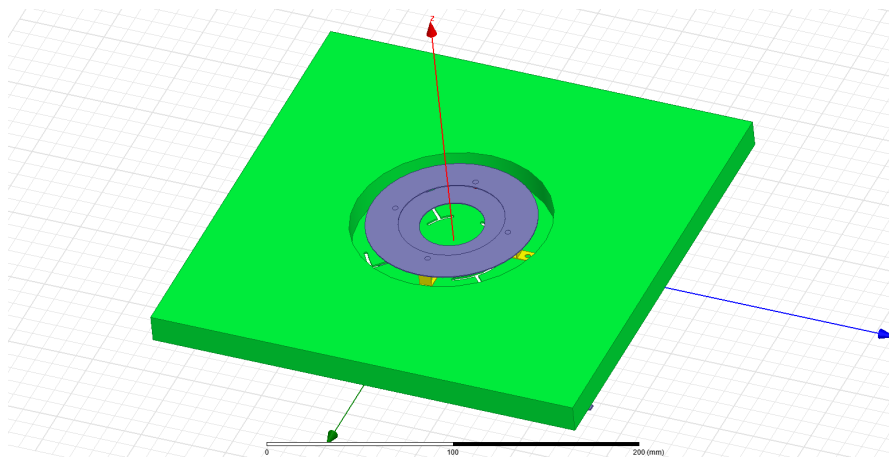


**Figure 4.26:** Old design, top view

For the first design the reflection coefficients can be seen in figures 4.28 and 4.29.

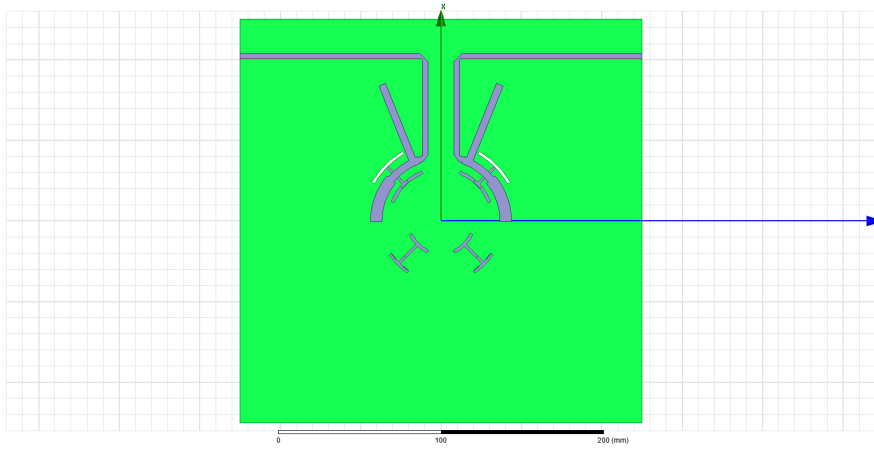


Figure 4.27: Old design, downside view

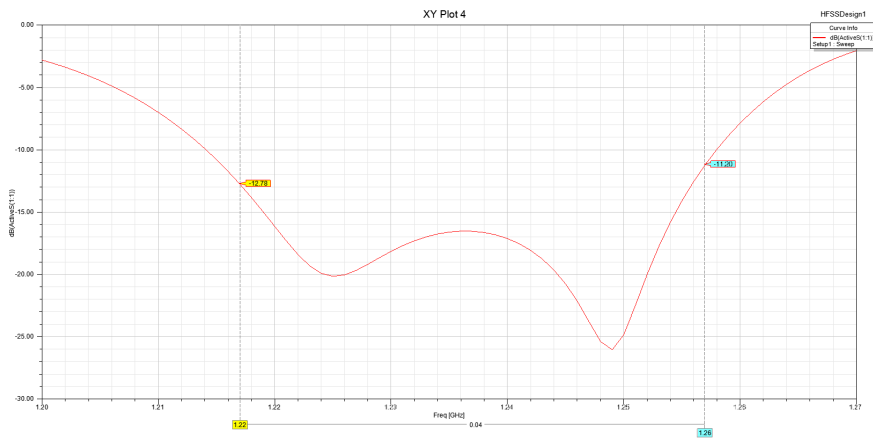


Figure 4.28: Low frequency design's S11

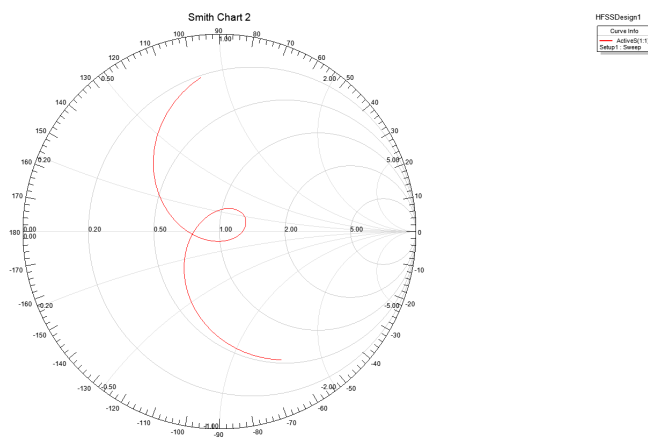
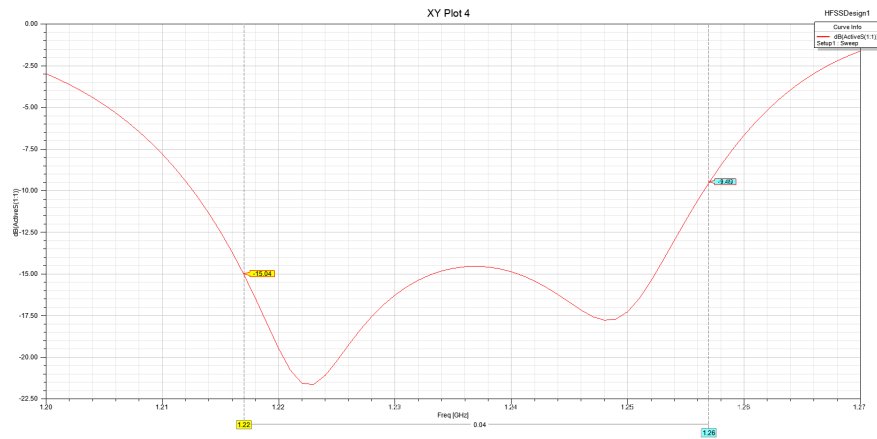
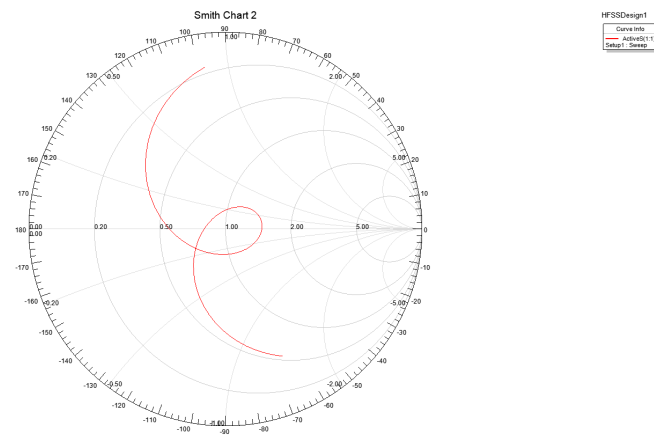


Figure 4.29: Low frequency design's reflection coefficient representation in the Smith Chart

The first thing that was done to this first design was to increase the height of the cavity. This way it was possible to add the third ring. But, for going step by step, first only the cavity height was changed to see how it affected the results. So, the first thing that was done, was to change the cavity height from 15mm to 17.45mm, in order to keep the same separation between the first and second ring and the second and the third ring. This separation is 2.45mm. So, making this change the obtained results are shown in figures 4.30 and 4.31. As can be seen, the change in height does not affect significantly to the overall design results.



**Figure 4.30:** Low frequency design's S11 after the height was changed



**Figure 4.31:** Low frequency design's reflection coefficient representation in the Smith Chart after the height was changed

Once this was done, the last thing that was needed was to add the third ring. The design with the third ring can be seen in figure 4.32. The results after adding the third ring are shown in figures 4.33 and 4.34. As can be seen the resonance is lost if the third ring was added.

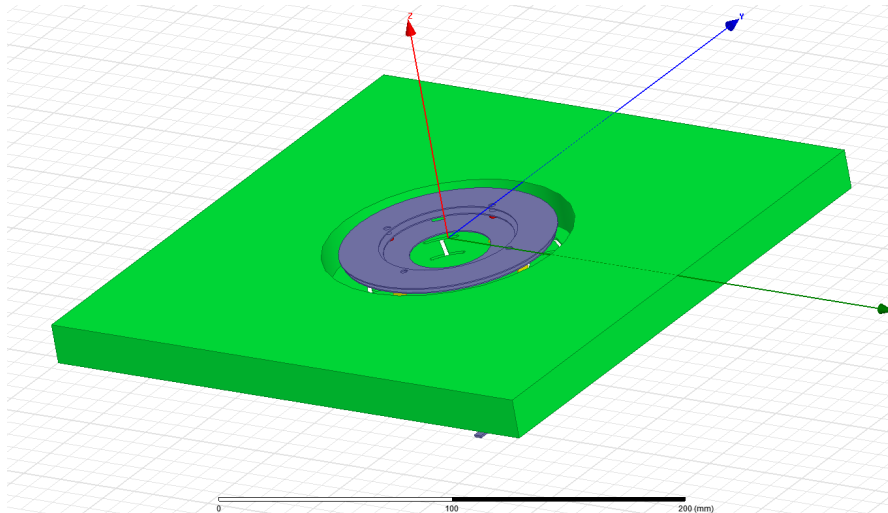


**Figure 4.32:** The previous design with the third ring added

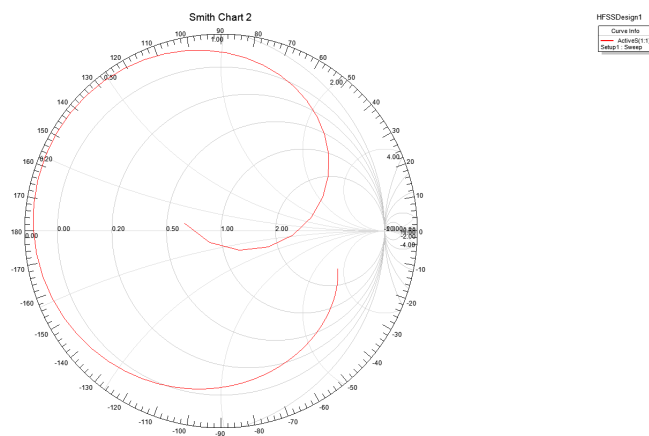


**Figure 4.33:** The S11 representation in the Smith Chart

If a broader simulation is done, the results could be seen in figure 4.35. As can be seen the resonance is lost.

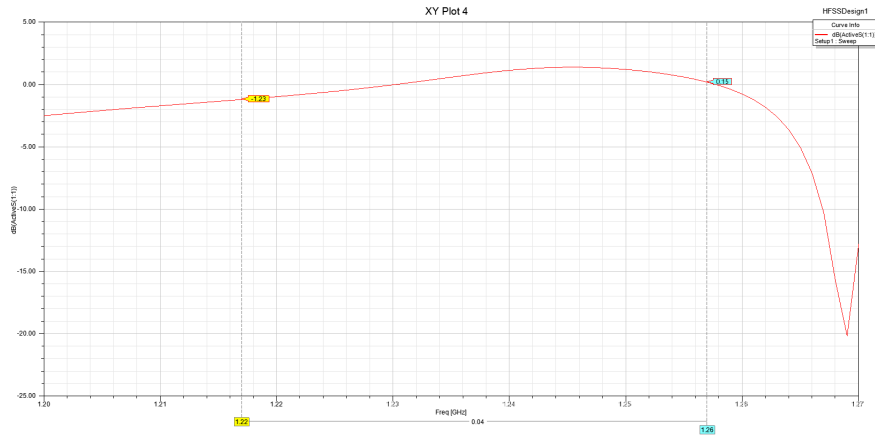


Figure 4.34: S11 with the third ring added

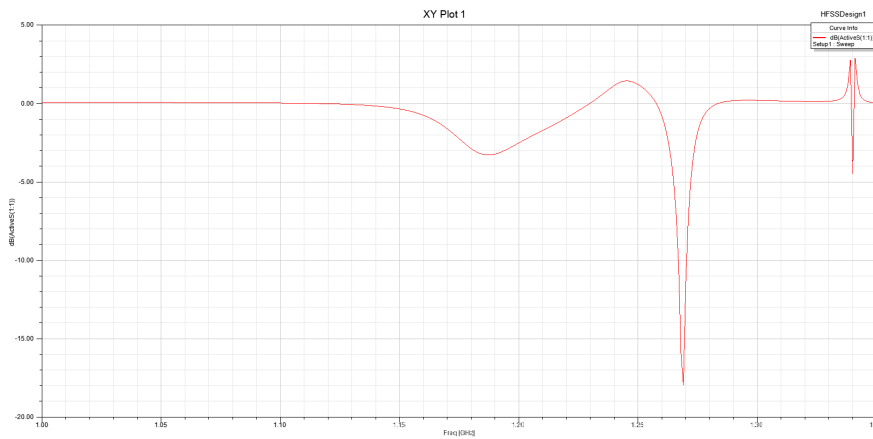
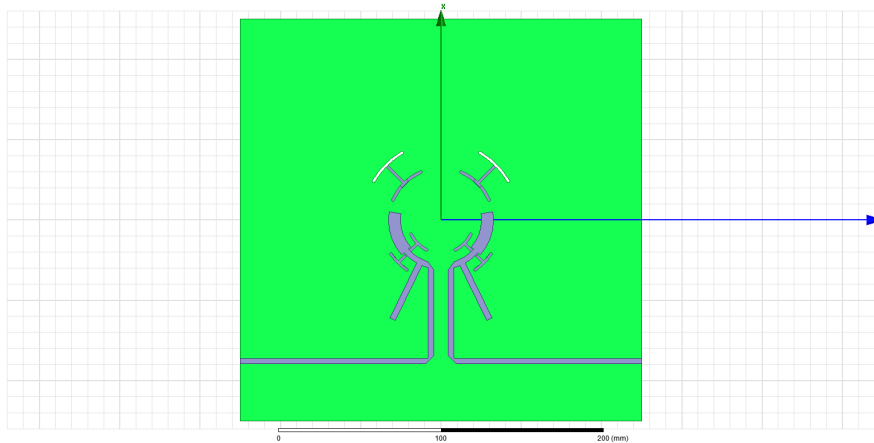
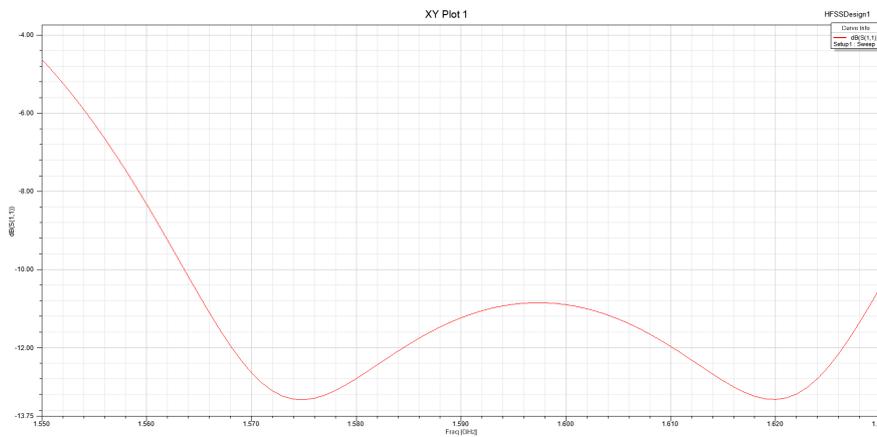


Figure 4.35: Same result but for a broader frequency range

For the high frequency, the same procedure was followed. First the cavity height was changed and then the third ring was added. The whole procedure will be avoided and only the final result with the third ring added will be shown. The results are shown in figures 4.35 and 4.36. As can be seen in those figures, the third ring does not affect that much the high frequency resonance.



**Figure 4.36:** The old design for the high frequency feeding



**Figure 4.37:** The previous design's S11 with the third ring added

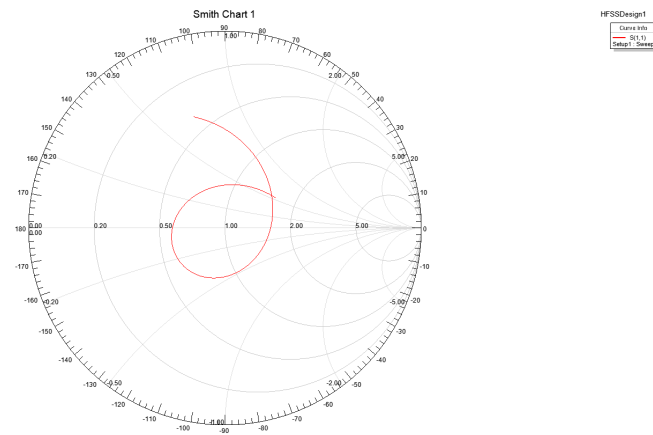


**Figure 4.38:** The previous design's  $S_{11}$  in the Smith Chart with the third ring added

If the same procedure is followed for the design where both feedings are together, as the one that can be seen in figure 4.39, similar results are found. The S11 plots can be seen in figure 4.40 for the high frequency and figure 4.41 for the low frequency. As can be seen, the third ring does not modify the high frequency while it has a huge impact in the low frequency resonance. The reason of this is that the third ring's resonance is very close to the second ring's resonance. Due to that, the coupling is very high and it is not possible to have good resonance. It can be concluded that to add the third ring it is not possible, at least for these frequency bands. Some other things were tried, like changing the height of the third ring, but they did not give any good results so the results are going to be avoided for this report.

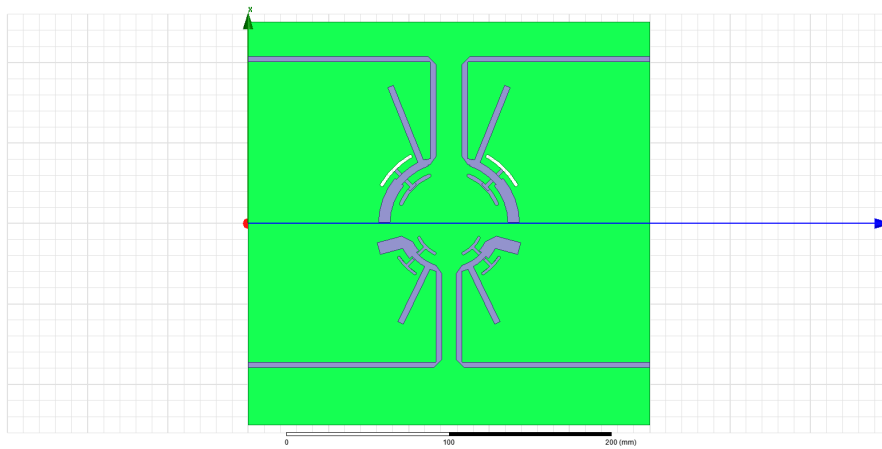


Figure 4.39: The old design for the high frequency feeding

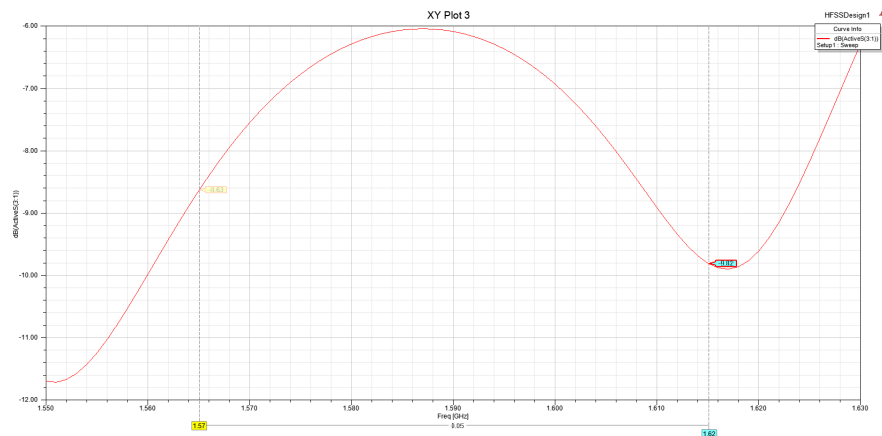
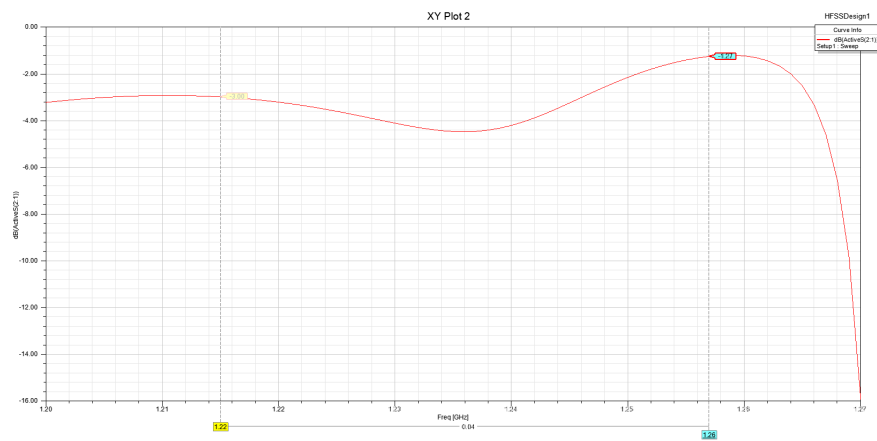


Figure 4.40: The previous design's S11 with the third ring added



**Figure 4.41:** The previous design's  $S_{11}$  in the Smith Chart with the third ring added

## 4.4 Same ring for L2 and L5

The next thing that was tried, was to try if it was possible to use the second ring for both the L2 and L5 frequency bands. In order to do so, the dimensions of the ring were changed. But what was seen doing that is that the resonant frequency was also changed as the ring dimensions were modified. What was seen is that the ring was the component that set the resonance frequency and it was not possible to change the rings resonance frequency by the feeding network. It could slightly be changed but the loop of the smith chart was move by the ring and not by anything else. So, this solution was dismissed as was seen that the resonant frequency was dependant on the ring. This resulted on the only possibility to excite the ring at a certain frequency, being impossible to excite the ring for two different frequency bands.

# 5

## New Antenna Design

**A**FTER the non succeeding solution proposals, what it was decided was to design an antenna for the L1 and L5 frequency bands, after seeing that a design for the three frequencies was not possible. In order to do so, the L2 matching of the previous design was tuned in order to have a resonance at 1.176GHz, the center frequency of the L5 frequency band. The design procedure will be explained in this chapter.

### 5.1 L5 Excitation

What was done in this part was to make the antenna resonate in the L5 frequency band. The center frequency, as said before, is at 1.176GHz. In order to do so, the outer and inner radiuses of the large ring were changed, from 28.3mm and 47.9 to 29.9mm and 50.9mm. Having this new ring, what it was done was to match the design again so the design had good matching. The design can be seen below, it can be seen that it is the same design as the old antenna design. First only with one slot excitation was tried. The design can be seen in figure 5.1. Having this design, the obtained reflection coefficient can be seen in figures 5.2 and 5.3. As can be seen, the antenna is matched around 1.176GHz, the wanted center frequency.

Once this first design was done, the second slot was excited, so we have a circular polarization. An image of the design can be seen in figure 5.4. With this second design, after making some changes in the stub and line length, the obtained reflection coefficients can be seen in figure 5.5 and 5.6. The matching for only one slot is shown because they both are very similar.

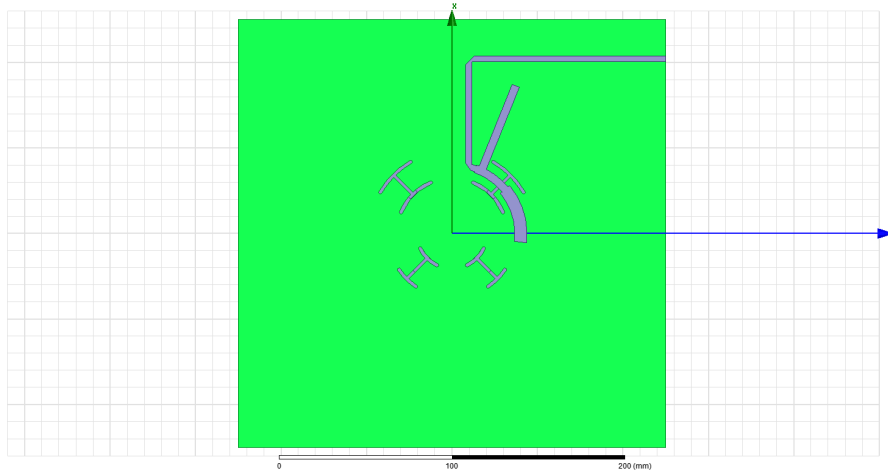


**Figure 5.1:** The first design for the L5 frequency band

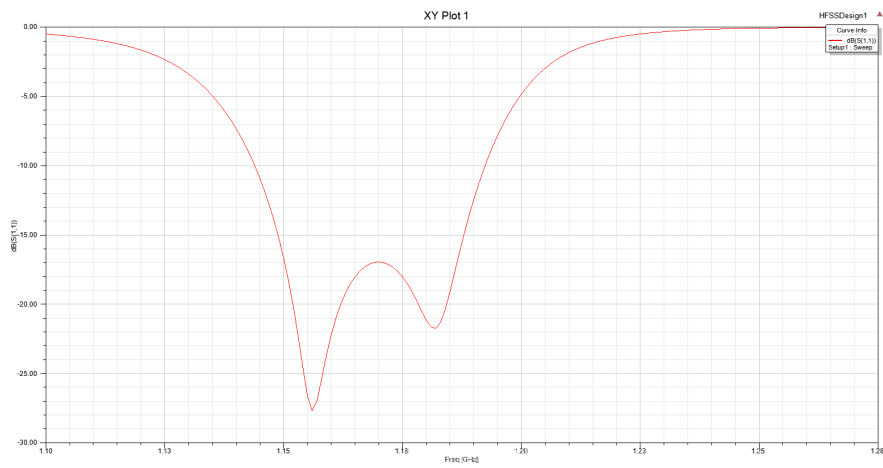


**Figure 5.2:** Reflection coefficient of the first design

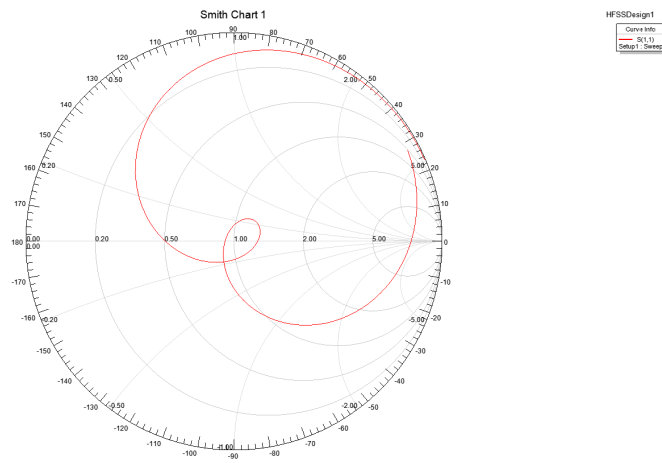


**Figure 5.3:** Reflection coefficient represented in the Smith Chart

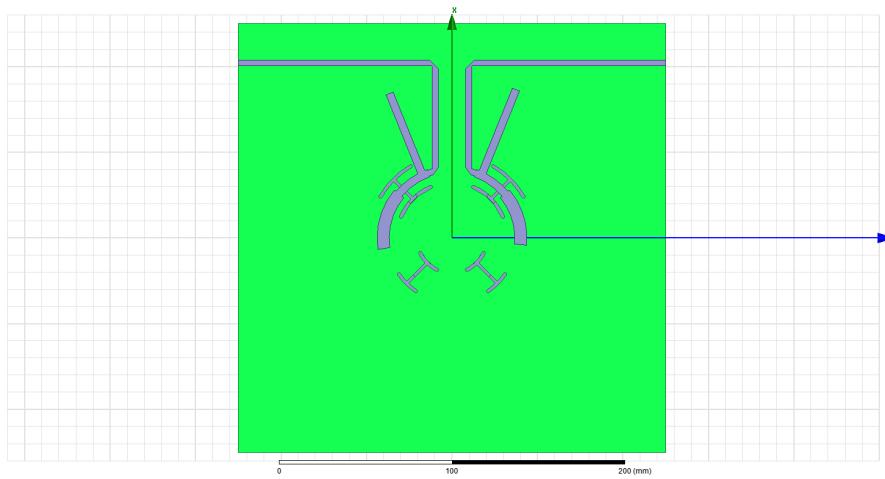


**Figure 5.4:** Excitation for both slots together

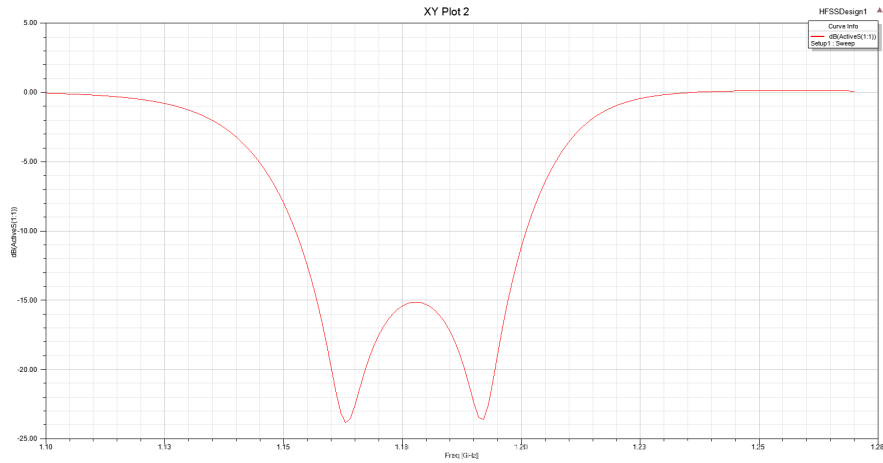


**Figure 5.5:** Reflection coefficient with both slots excited

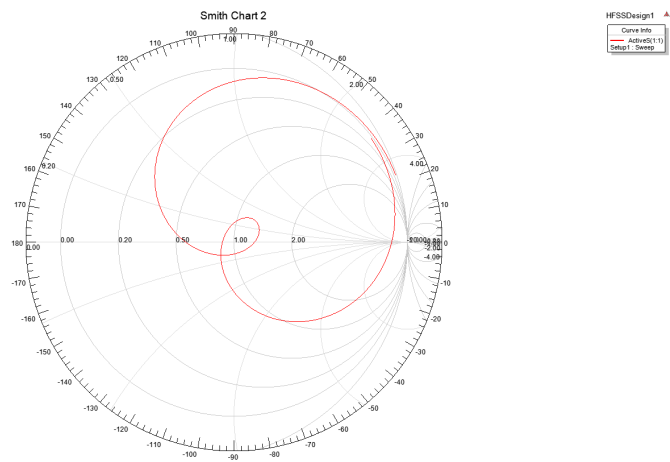


**Figure 5.6:** Reflection coefficient represented in the Smith Chart

Once this was done the whole design was put together. A picture of the design can be seen in figure 5.7. It can be seen that all the slots were added. Besides, a bending was added to the low frequency slots in order to fit the design in space. For that a miter as explained in chapter 2 was used. For the high frequency the reflection coefficient is plotted in figures 5.8 and 5.9. With this designs, the co and cross-polar polarizations can be seen in figure 5.10 and figure 5.11, at the center frequency.

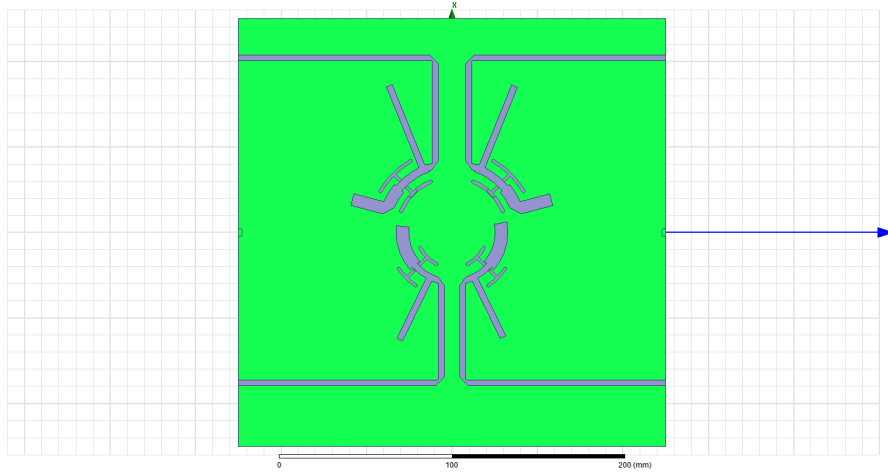


Figure 5.7: Excitation for both slots together

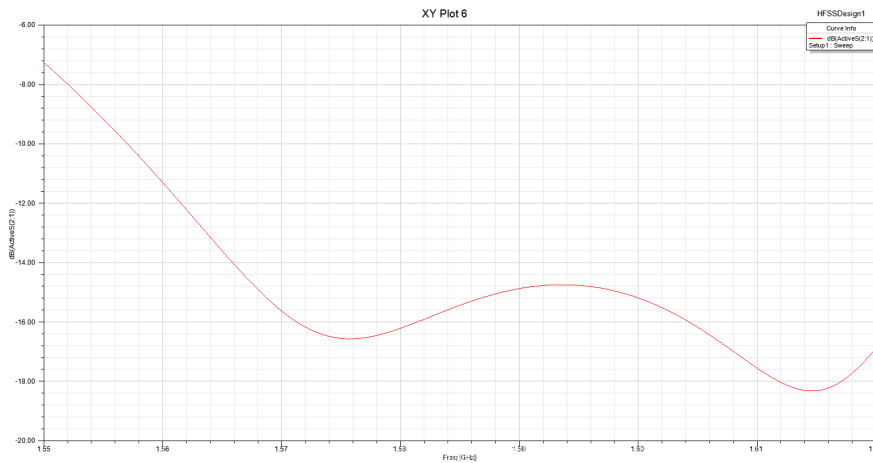


Figure 5.8: Reflection coefficient for the L1 band

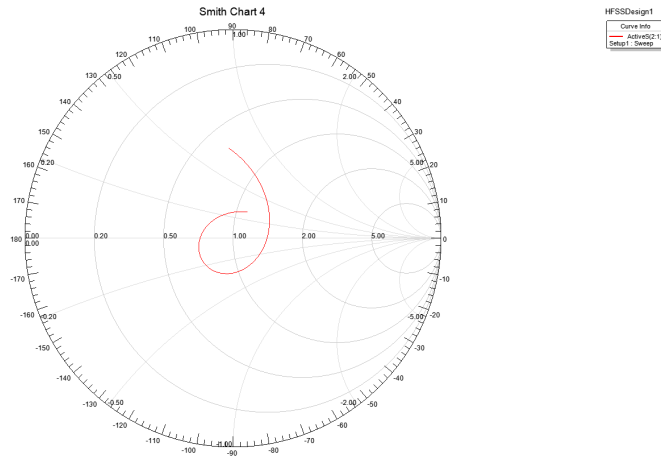


Figure 5.9: Reflection coefficient represented in the Smith Chart

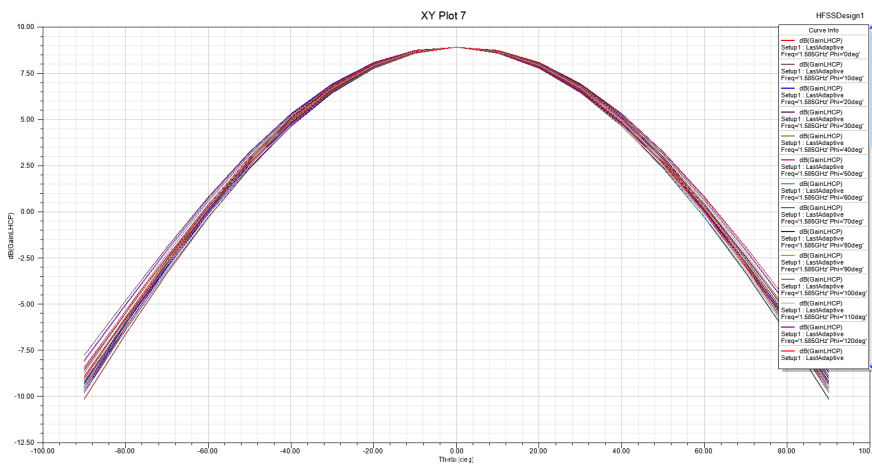


Figure 5.10: Co-polar pattern for the L1 band at center frequency

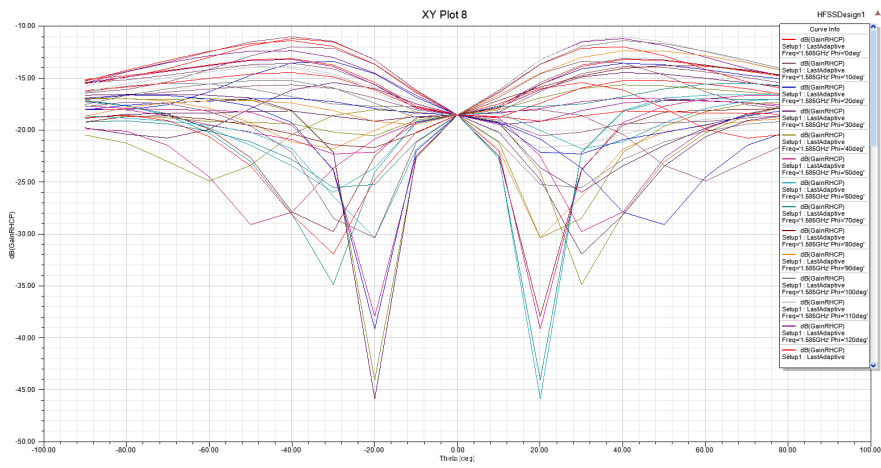


Figure 5.11: Cross-polar pattern for the L2 band at center frequency

While for the lower frequency the reflection coefficient values can be seen in figures 5.12 and 5.13. The co-polar and the cross-polar values, in the other hand, can be seen in figure 5.14 and figure 5.15. It can be seen that the matching is fairly good for the two frequencies. So, the next step is to add a quarter wavelength pice of line in both of the frequency bands. This is going to be the last step of this Master thesis, to add the quarter wavelength pice between the two pieces of line in order to have the 90 degree difference between the two slots. This is going to be shown in the next section.

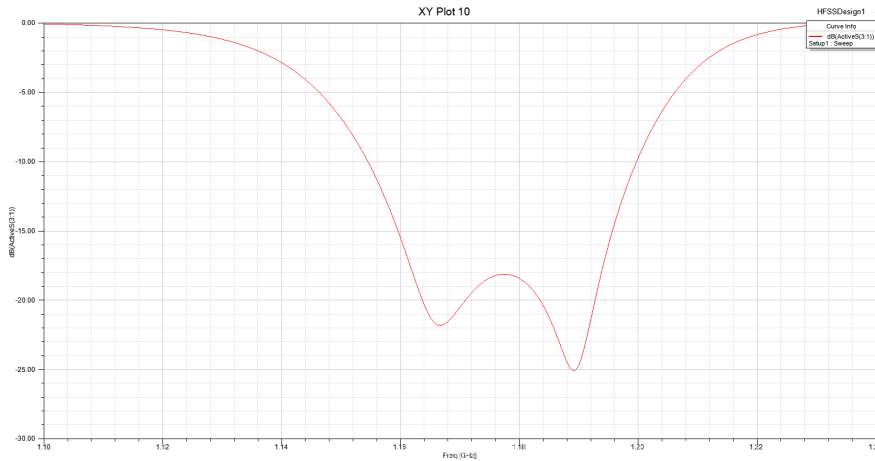


Figure 5.12: Reflection coefficient for the L5 band

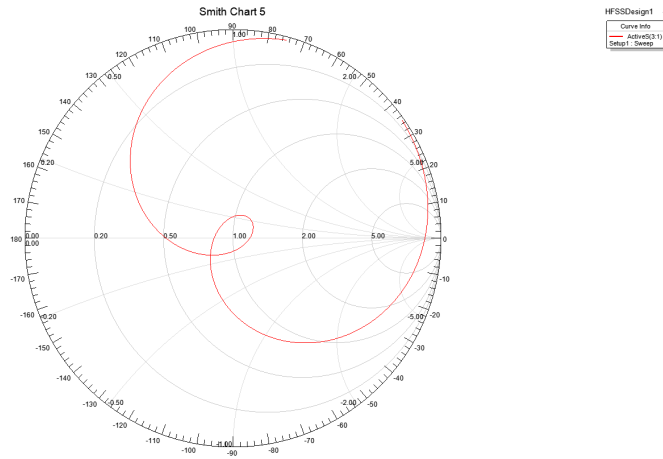


Figure 5.13: Reflection coefficient represented in the Smith Chart

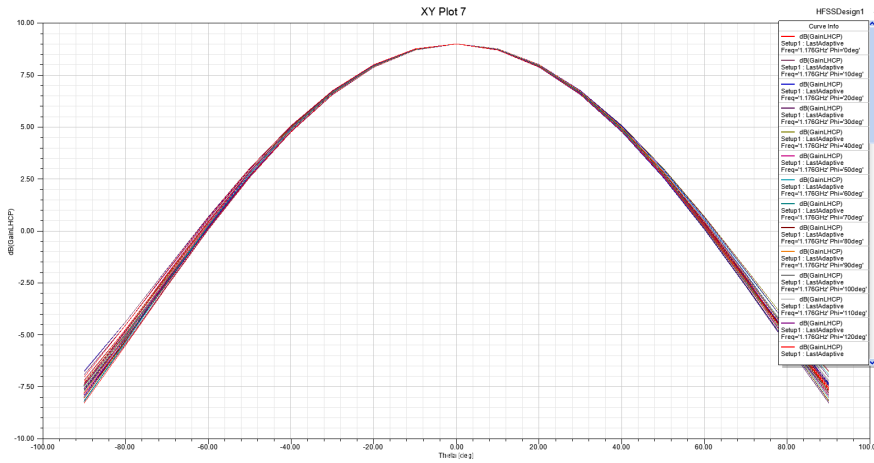


Figure 5.14: Co-polar pattern for the L5 band at center frequency

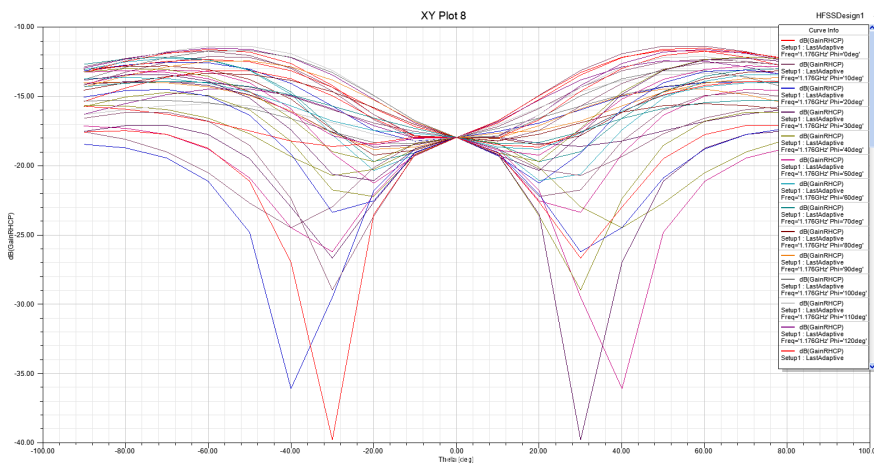
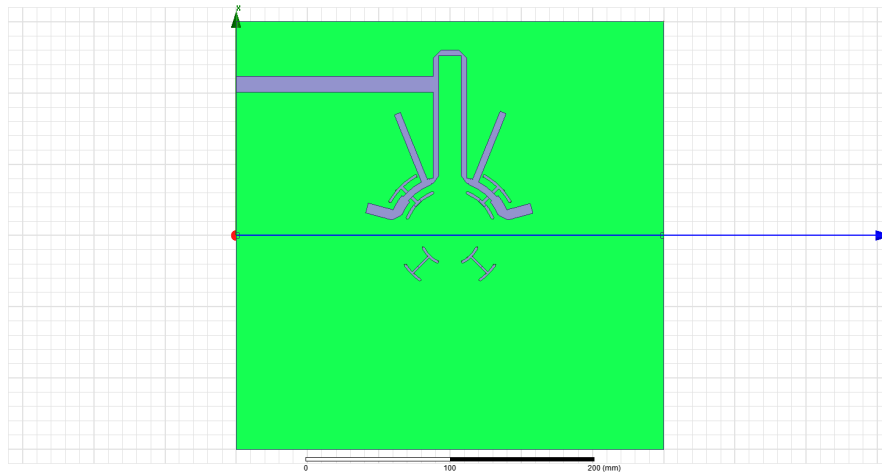


Figure 5.15: Cross-polar pattern for the L2 band at center frequency

## 5.2 Design lambda/4 line

After the design with the four ports is obtained, the following step is to have only one port for each frequency band, add the quarter wavelength line between port 1 and port 2 in order to have the 90 degrees difference among the ports. The design was started from the L5 frequency band feeding network. The both ports were put together in the way that can be seen in figure 5.16. As can be seen, the signal goes from a wide line and is separated into two narrower lines. This is a T junction power divider. The power divider works as follows; The line that has  $Z_0$  of 42.5 ohm (11.2mm wide) is divided into two lines that have 85ohm (3.5mm wide lines). This is the principle of a T power divider, the lines where the power is divided need to have two times the impedance of the main line. So usign this power divider the signal is divided into two lines. In order to have 90 degrees difference between the two slots, a quarter wavelength piece of line is added to the design, being a piece of line of 63mm. It can be seen in the figure that htere is an extra line length in the design.



**Figure 5.16:** Reflection coefficient for the L5 band

Having this design, the reflection coefficient values for the lower frequency band (L5) can be seen in figures 5.17 and 5.18. For this reflection coefficient, the co-polar and cross-polar pattern of the antenna can be seen in figure 5.19 and 5.20, for the center frequency of 1176GHz.

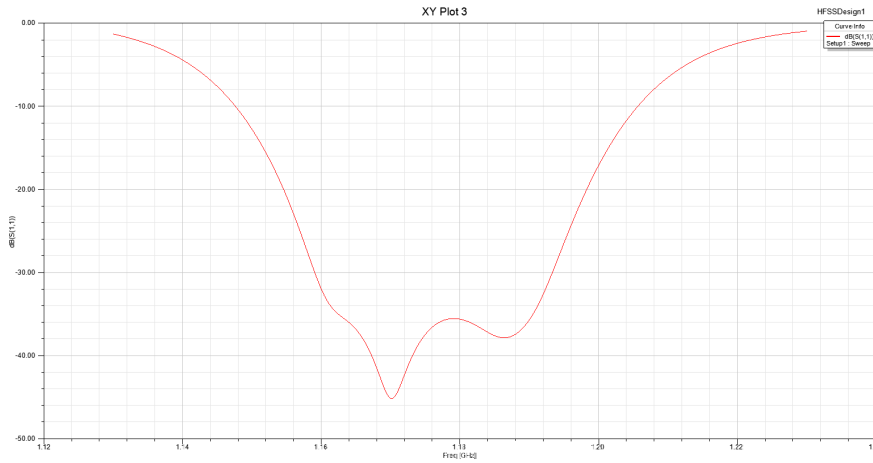


Figure 5.17: Reflection coefficient for the L5 band with the quarter wavelength line

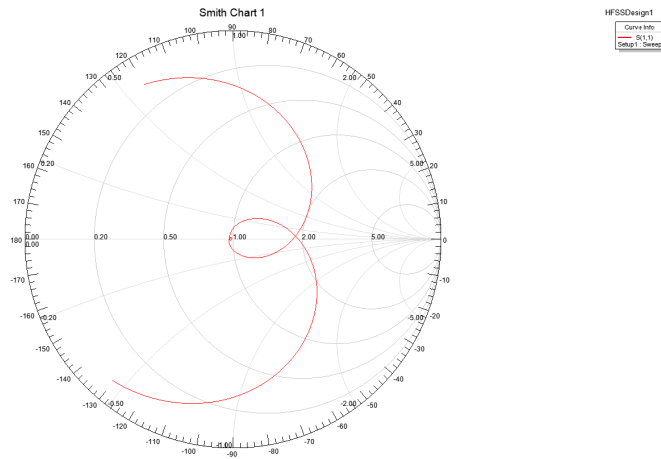


Figure 5.18: Reflection coefficient represented in the Smith Chart

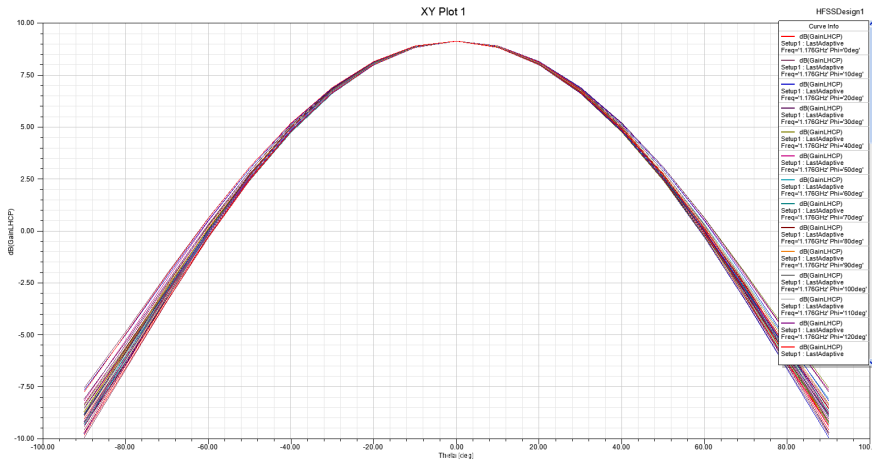


Figure 5.19: Co-polar pattern for the L5 band at center frequency

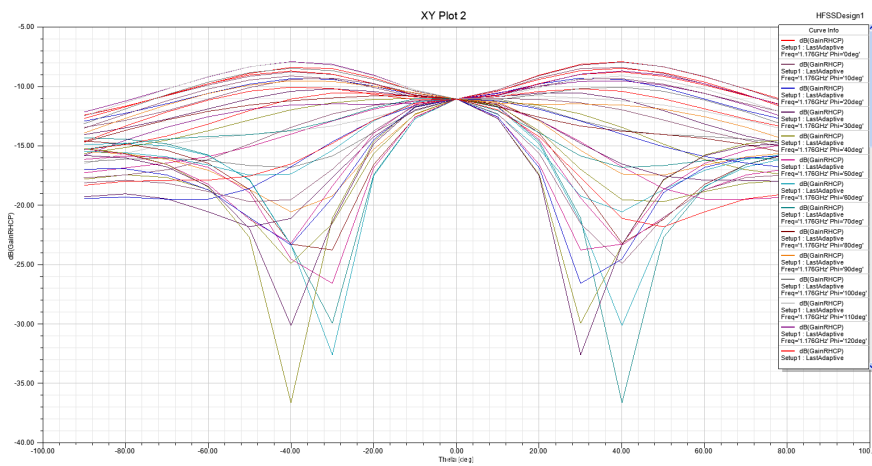
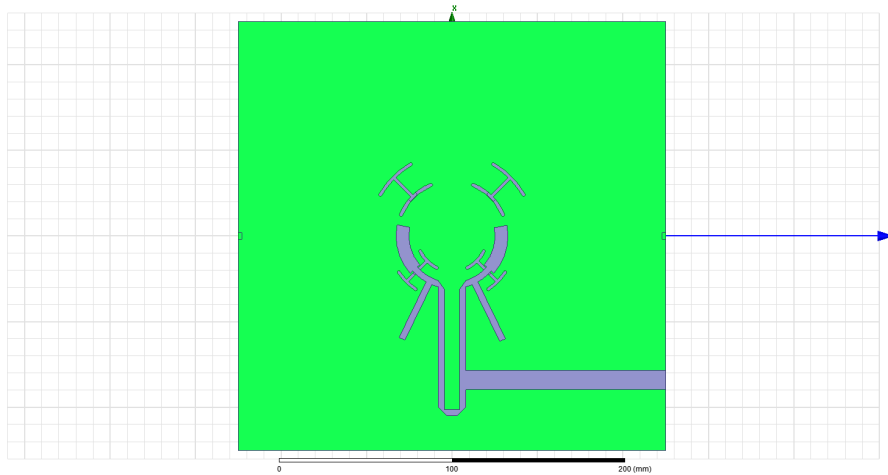
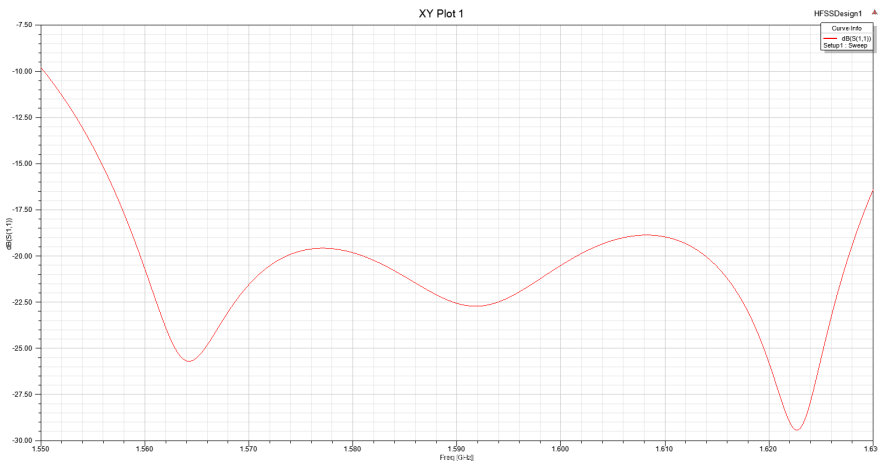


Figure 5.20: Cross-polar pattern for the L5 band at center frequency

For the higher frequency band the procedure is the same. A quarter wavelength piece of line is added to the design as in the previous one. In this case, the length of the quarter wavelength line's length is 47mm. A picture of the design can be seen in figure 5.21. Having such a design, the reflection coefficient values can be seen in figures 5.22 and 5.23, while in figures 5.24 and 5.25 the radiation patterns of the antenna can be seen. It can be said that, after adding the quarter wavelength line, the matching of the antenna is improved. This could be due to the internal reflections in the feeding network.



**Figure 5.21:** Reflection coefficient for the L1 band



**Figure 5.22:** Reflection coefficient for the L1 band with the quarter wavelength line

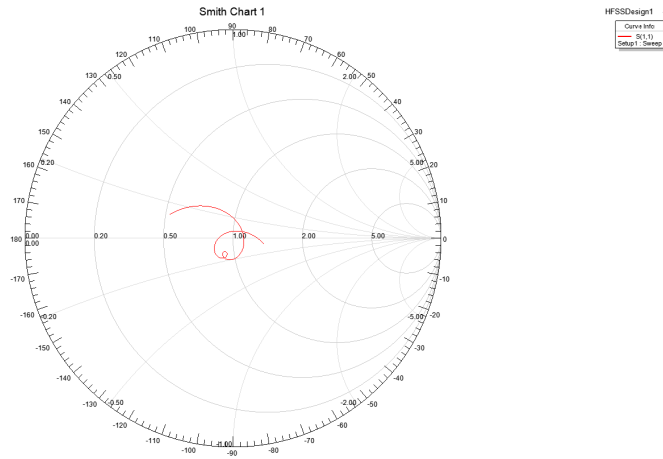


Figure 5.23: Reflection coefficient represented in the Smith Chart

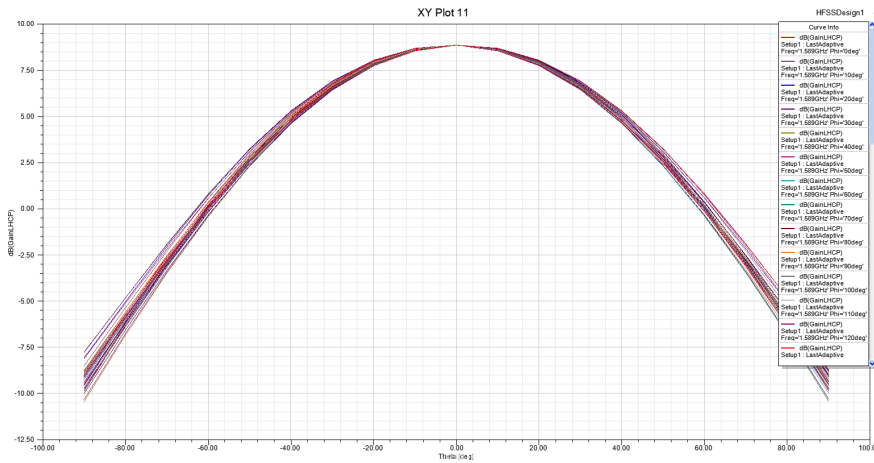


Figure 5.24: Co-polar pattern for the L1 band at center frequency

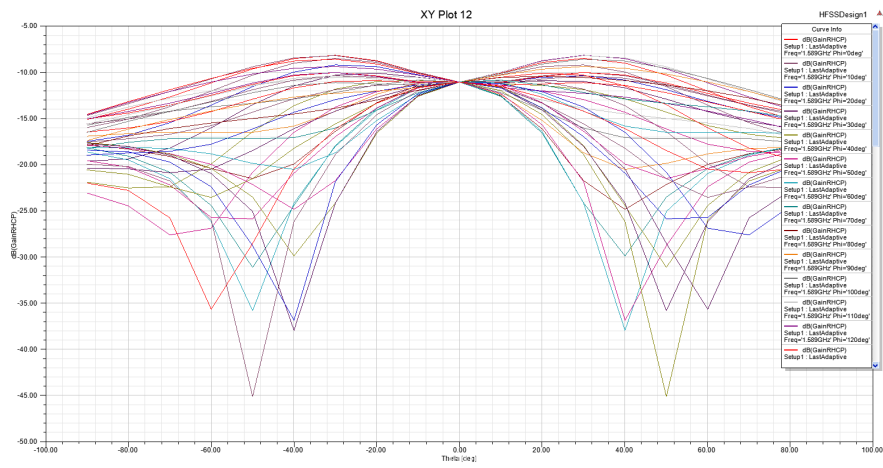


Figure 5.25: Cross-polar pattern for the L1 band at center frequency

### 5.3 Final Design

After adding the quarter wavelength line to both frequency bands, the last thing that is left is to put both feeding networks together. This is what was done last. A picture of the final design can be seen in figure 5.26. Having this design the reflection coefficient and the radiation pattern figures for the lower frequency band can be seen in the figures from 5.27 to 5.31. For the higher frequency band, in the other hand, can be seen in figures coming from 5.32 to 5.36. It can be seen that the radiation patterns for the frequencies far the center is not as good as in the center. This is because of the fact that a quarter wavelength for these frequencies is different that for the center frequency.

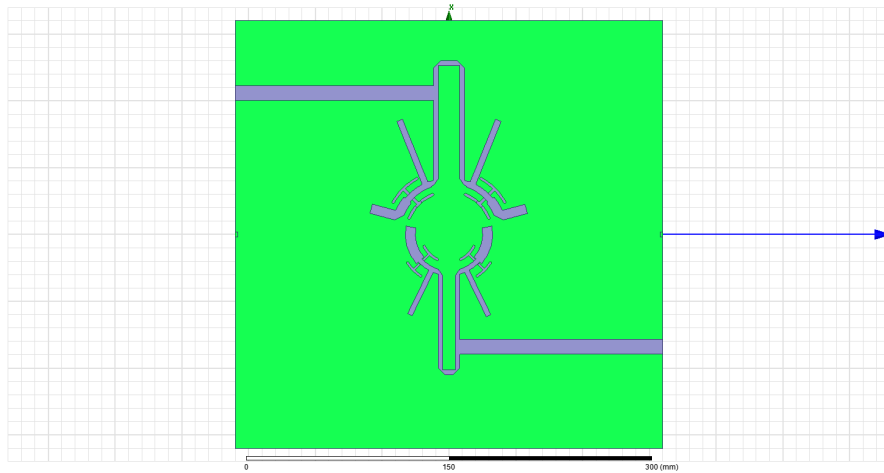


Figure 5.26: Final design picture

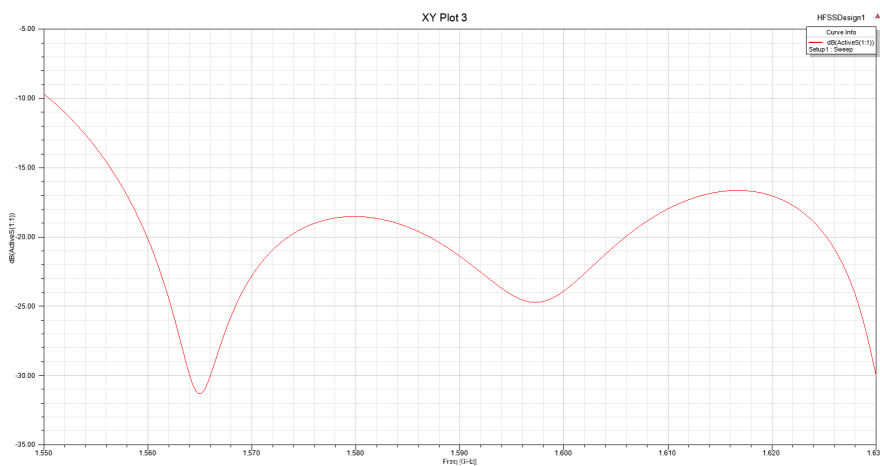


Figure 5.27:  $S_{11}$  for the lower frequency band

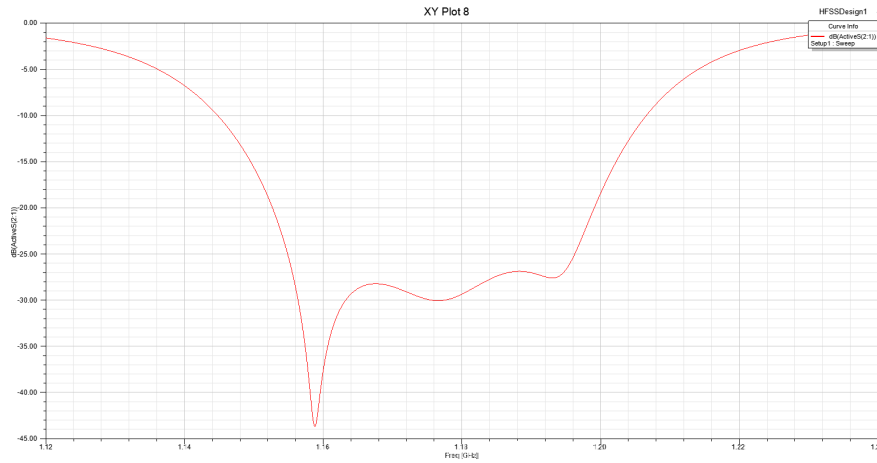


Figure 5.28: Reflection coefficient in Smith Chart for the lower frequency band

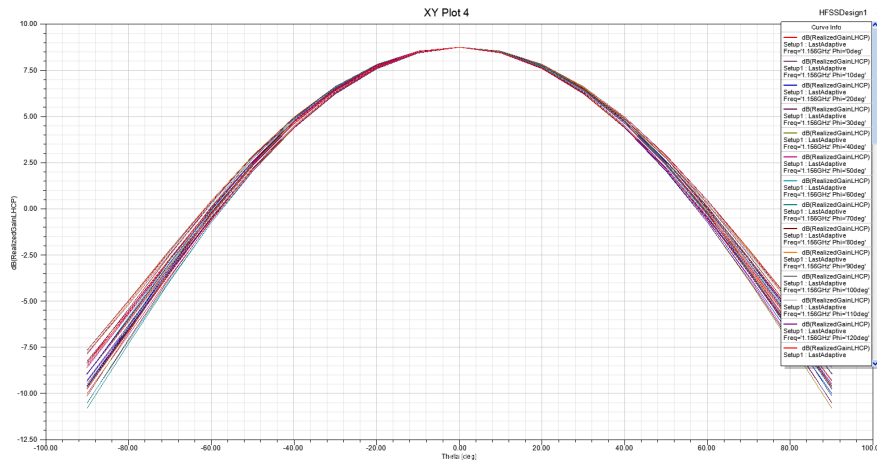


Figure 5.29: Radiation pattern at 1156MHz

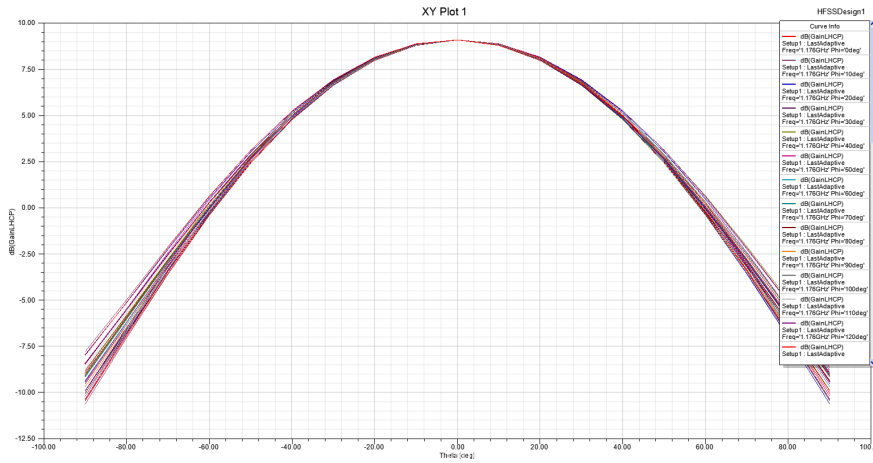


Figure 5.30: Radiation pattern at 1176MHz

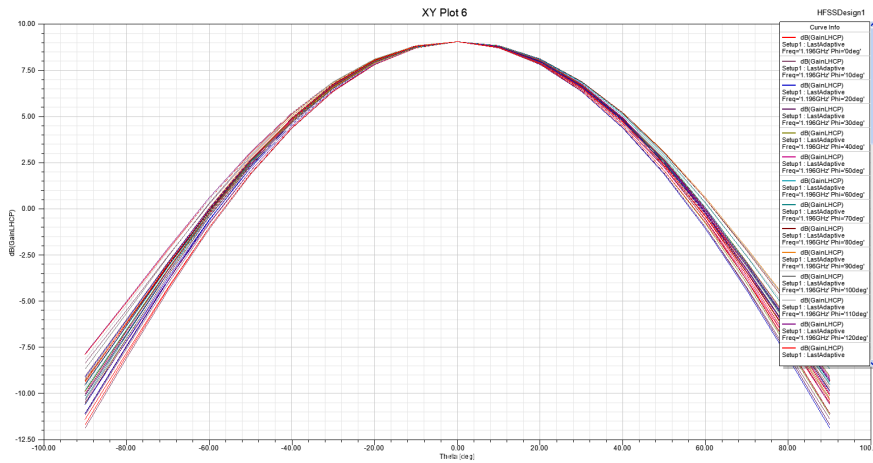


Figure 5.31: Radiation pattern at 1196MHz

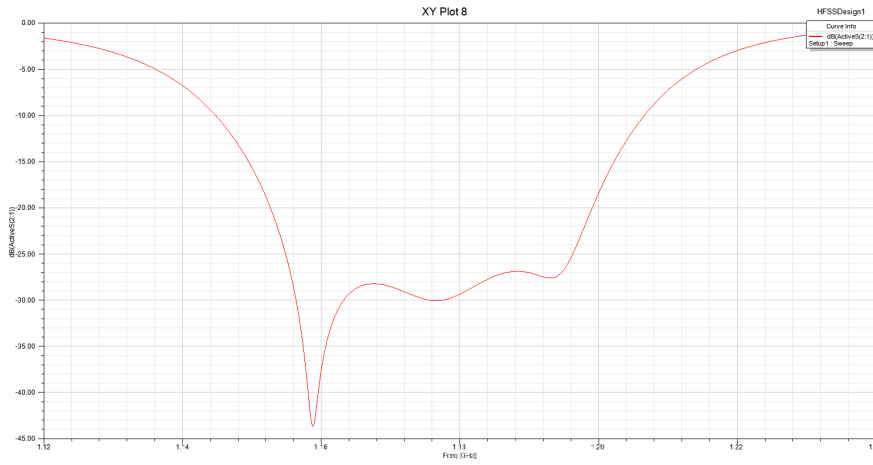


Figure 5.32:  $S_{11}$  for the larger frequency band

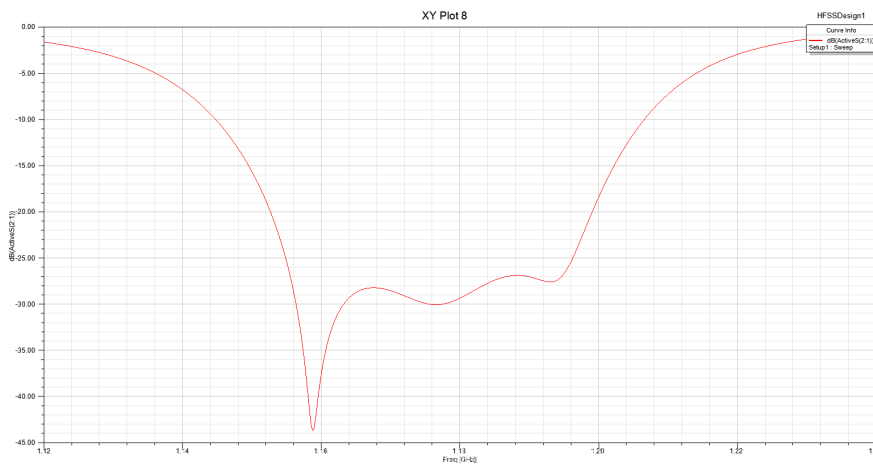


Figure 5.33: Reflection coefficient in Smith Chart for the larger frequency band

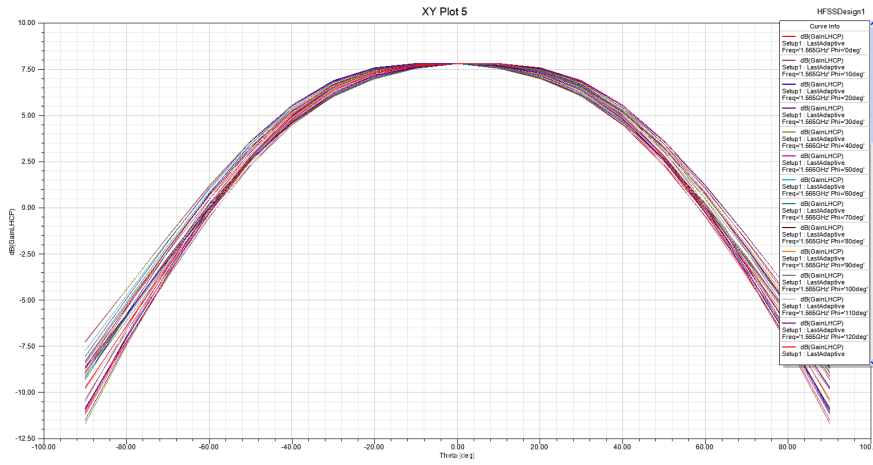


Figure 5.34: Radiation pattern at 1565MHz

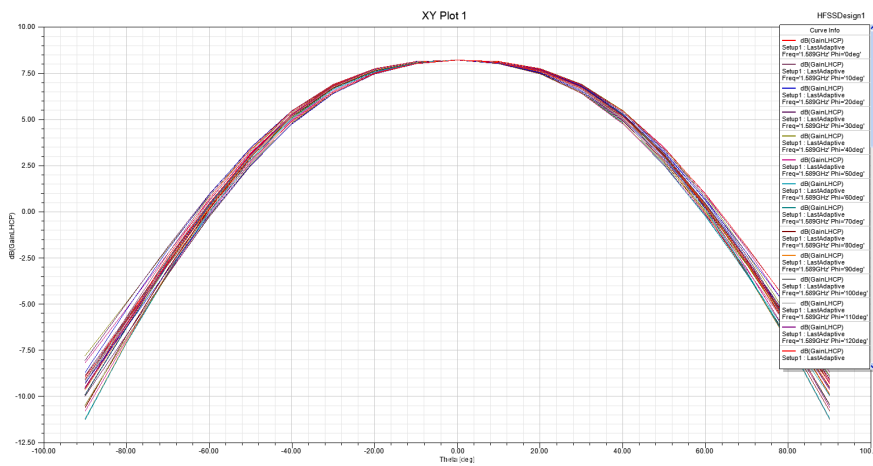


Figure 5.35: Radiation pattern at 1589MHz

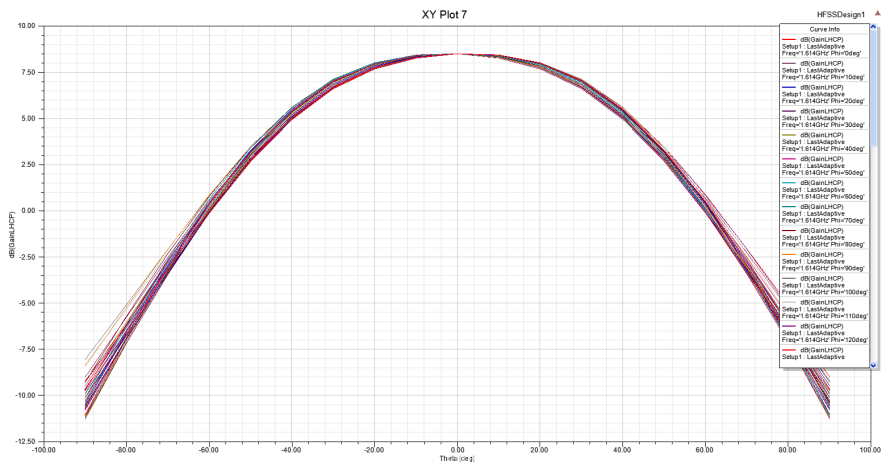


Figure 5.36: Radiation pattern at 1614MHz

## 5.4 Conclusions

As a conclusion it can be said that there are two main limitations for this antenna. The first one is that the antenna is a narrowband antenna. As it was seen during the design process, the antenna has a bandwidth of 50MHz, which means that the antenna is very narrowband. It was tried to increase this bandwidth but it was impossible to increase it. The second limitation is the cross polaritation level. As it can be seen, the cross polarization is also very high in part of the frequency band. After this study, it can be said that this antenna can be used in applications where this two facts are not very important.

# Bibliography

- [1] RUAG Space AB Sweden, RUAG Space AB Sweden.  
URL <http://www.ruag.com/space/ruag-space-sweden/>
- [2] RUAG Space AB Sweden, Media Release (October 2014).  
URL [https://en.wikipedia.org/wiki/Radio\\_occultation](https://en.wikipedia.org/wiki/Radio_occultation)
- [3] Ansys HFSS, High Frequency Electromagnetic simulator.  
URL <http://www.ansys.com/Products/Electronics/ANSYS-HFSS>
- [4] Wikipedia, Radio Occultation.  
URL [https://en.wikipedia.org/wiki/Radio\\_occultation](https://en.wikipedia.org/wiki/Radio_occultation)
- [5] R. Olsson, P.-S. Kildal, S. Weinreb, The Eleven antenna: a compact low-profile decade bandwidth dual polarized feed for reflector antennas, *Antennas and Propagation, IEEE Transactions on* 54 (2) (2006) 368–375.
- [6] A. Yasin, J. Yang, T. Ostling, A novel compact dual band feed for reflector antennas based on choke horn and circular Eleven antenna, *IEEE Trans. on Antennas Propagat.* 57 (10) (2009) 3300–3302.
- [7] J. Yin, J. Yang, M. Pantaleev, L. Helldner, The circular Eleven antenna: a new decade-bandwidth feed for reflector antennas with a high aperture efficiency, *IEEE Trans. on Antennas Propagat.* 61 (8) (2013) 3976–3984.
- [8] Jian Yang, M. Pantaleev, B. Billade, M. Ivashina, T. Carozzi, L. Helldner, Leif and M. Dahlgren, A Compact Dual-Polarized 4-Port Eleven Feed With High Sensitivity for Reflectors Over 0.35–1.05 GHz, *IEEE Trans. on Antennas Propagat.* 63 (12) (2015) 5955–5960.
- [9] P.-S. Kildal, R. Olsson, J. Yang, Development of three models of the Eleven antenna: a new decade bandwidth high performance feed for reflectors, 1st Eur. Conf. on Antennas Propagat. (EuCAP2006), 6 - 10 November 2006.

- [10] Jian Yang, Miroslav Pantaleev, Truly Conical Eleven Antenna: a New Geometry for Applications at High Frequencies, 2016 IEEE AP-S International Symposium, June 25-July 1, 2016.
- [11] J. Yang, A. Kishk, A novel low-profile compact directional ultra-wideband antenna: the self-grounded Bow-Tie antenna, *IEEE Trans. on Antennas Propagat.* 60 (3) (March 2012) 1214–1220.
- [12] Yinan Yu, Jian Yang, Tomas McKelvey, Borys Stoew, A Compact UWB Indoor and Through-Wall Radar with Precise Ranging and Tracking, *International Journal on Antenna and Propagations* 2012 (Article ID 678590) (2012) 11 pages.
- [13] Hasan Raza, Ahmed Hussain, Jian Yang, Per-Simon Kildal, Wideband Compact 4-Port Dual Polarized Self-Grounded Bowtie Antenna, *IEEE Trans. on Antennas Propagat.* 62 (9) (Sept 2014) 4468–4473.
- [14] Shirin Abtahi, Jian Yang, Stefan Kidborg, A new compact multiband antenna for stroke diagnosis system over 0.5-3 GHz, *Microwave and Optical Technology Lett.* 54 (10) (Oct 2012) 2342–2346.
- [15] Sadegh Mansouri Moghaddam, Andres Alayon Glazunov, Jian Yang, Mattias Gustafsson, Per-Simon Kildal, Comparison of 2-bitstream polarization-MIMO performance of 2 and 4-port bowtie antennas for LTE in random-LOS, 2015 International Symposium on Antennas and Propagation (ISAP).
- [16] P.-S. Kildal, The hat feed: a dual-mode rear-radiating wave-guide antenna having low cross-polarization, *IEEE Trans. Antennas Propag.* 35 (9) (1987) 1010–1016.
- [17] J. Yang and P.-S. Kildal, FDTD design of a Chinese hat feed for shallow mm-wave reflector antennas, *IEEE Antennas and Propagation Society International Symposium* 4 (1998) 2046–2049.
- [18] M. Denstedt, T. Ostling, J. Yang and P.-S. Kildal, Tripling bandwidth of hat feed by genetic algorithm optimization, In *Proc. 2007 IEEE AP-S International Symposium*, June 10-15, 2007.
- [19] Erik G. Geterud, Jian Yang, Tomas Ostling, and Pontus Bergmark, Design and optimization of a compact wideband hat-fed reflector antenna for satellite communications, *IEEE Trans. Antenna Propagat.* 61 (1) (2013) 125–133.
- [20] E. G. Geterud, J. Yang and T. Östling, Wide band hat-fed reflector antenna for satellite communications, In *5th Eur. Conf. on Antennas Propagat. (EuCAP2011)*, 11 - 15 April 2011.
- [21] E. Geterud, J. Yang and T. Ostling, Radome Design for Hat-Fed Reflector Antenna, *6th Eur. Conf. on Antennas Propagat. (EuCAP2012)*, 26-30 March 2012.

- [22] Wei Wei, Jian Yang, Tomas Ostling and Thomas Schafer, A new hat feed for reflector antennas realized without dielectrics for reducing manufacturing cost and improving reflection coefficient, *IET Microwaves Antennas Propagat* 5 (7) (July 2011) 837–843.
- [23] Jian Yang, Jonas Flygare, Miroslav Pantaleev and Bhushan Billade, Development of Quadruple-ridge Flared Horn with Spline-defined Profile for Band B of the Wide Band Single Pixel Feed (WBSPF) Advanced Instrumentation Programme for SKA, 2016 IEEE AP-S International Symposium, June 25-July 1, 2016.
- [24] ESA, GEROS-ISS project (March 2015).  
URL [http://www.esa.int/Our\\_Activities/Observing\\_the\\_Earth/](http://www.esa.int/Our_Activities/Observing_the_Earth/)
- [25] Saab Ericsson Aerospace, GRAS ANTENNA; Technical Data Package, Tech. rep., RUAG Space AB Sweden (2000).
- [26] David M. Pozar, *Microwave Engineering*, Wiley, United States of America, 1998.
- [27] Per-Simon Kildal, *Foundations of Antenna Engineering*, Kildal, Gothenburg, Sweden, 2015.